Hybrid Fuel Cell for Mobile Devices: An Integrated Approach

by

Munhee Sohn

S.B., Mechanical Engineering
Massachusetts Institute of Technology, 2004

Submitted to the Department of Mechanical Engineering
in Partial Fulfillment of the Requirements for the Degree of

Master of Science in Mechanical Engineering

at the

Massachusetts Institute of Technology

June 2006

Signature of Author .....
Department of Mechanical Engineering
May 12, 2006

Certified by .....
Jung-Hoon Chun
Professor of Mechanical Engineering
Thesis Supervisor

Accepted by .....
Lallit Anand
Professor of Mechanical Engineering
Chairman, Department Committee on Graduate Students

This page intentionally left blank

Hybrid Fuel Cell for Mobile Devices: An Integrated Approach

by

Munhee Sohn

Submitted to the Department of Mechanical Engineering on May 12, 2006
in Partial Fulfillment of the Requirements for the Degree of
Master of Science in Mechanical Engineering

ABSTRACT

As mobile devices advance to 3G and beyond, there will be a pressing need for increased power to drive these devices, which the current batteries cannot provide. The direct methanol fuel cell has been identified as a promising candidate to provide power to future mobile devices. However, commercialization of mobile devices containing fuel cells has been difficult due to several factors, including inefficiencies in the fuel cell, its large size, and difficulties of integration into the device. An Axiomatic approach was used to identify the key problems that prevent commercialization, along with identifying possible solutions for these problems. These possible solutions were investigated for use in developing a fuel cell for mobile devices of high performance, small size, and integrated hybrid circuitry.

To construct a high performance fuel cell, several experiments varying the methanol flow rate, oxygen and methanol concentration, and cathode gas diffusion layer (GDL) were performed on two standard membrane electrode assemblies (MEA). In addition, an MEA was modified using polyvinyl alcohol (PVA) to test its effect on decreasing methanol crossover for improved fuel cell performance. In order to decrease the overall size of the fuel cell, a passive fuel cell design was implemented.

A potentionstat was used to measure voltage and current and these measurements were used to plot current and power density curves. These results showed that increasing oxygen concentration improved performance, whereas increasing methanol concentration decreased performance due to methanol crossover effects. The effects of the changes of methanol flow rates were negligible and using a plain carbon cloth was just as efficient as using carbon paper coated with a micropourous layer. The performance of the prefabricated MEAs was much lower than that of the experimentally fabricated MEAs, but followed normal performance curve trends. Furthermore, the modified PVA/Nafion membrane showed improvement in preventing methanol crossover although it had decreased proton conductance. Finally, a fuel cell – capacitor hybrid circuit demo was designed and demonstrated.

Thesis supervisor: Jung-Hoon Chun
Title: Professor of Mechanical Engineering

This page intentionally left blank

Acknowledgements

First and foremost, I want to thank and praise God for His faithfulness throughout all of my life, but especially my time at MIT. For without Him, none of this would have been possible.

I would like to thank my parents for their love and sacrifice, and all of my family for always being there for me.

I would like to thank my advisor, Professor Jung-Hoon Chun, for the opportunity to work in his lab and for his guidance throughout my graduate research.

I would also like to thank my colleagues of 35-332 and 35-135 for their friendship. Special thanks goes to Kunal Thaker and Grant Shoji for giving up their time to help me use their hot press machine. I also really appreciated Victor Sinow for helping me with the hybrid circuitry. And to my friends Albert Lin and Ryan Huang, I thank them for sharing their expertise in their respective fields with me. Sam- thanks for being my labmate.

I would also like to thank the staff of the LMP shop, Dr. Barbara Hughey, Dr. JaeHyuk Jang from Samsung Electro-mechanics, and Chairman Moohyun Lim from Dae Joo Electronic Materials for the various ways they supported my research.

I want to thank all of my friends for their support and prayer, and want to acknowledge two people who are very dear to me. Sarah, you have been a great roommate, a wonderful friend, and a beautiful sister in Christ. I will miss you dearly next year. Youngmin, thank you for always believing in me. I love you, and I can't wait to start a new life together with you.

Finally, I would like to thank KIMM for their help, especially Dr. Changrae Lee for answering my numerous questions, and the KIMM-MIT alliance for funding this work.

In loving memory of my grandfather, Naekyun Shin, who was always proud of me.

This page intentionally left blank

Table of contents

List of figures

List of tables

CHAPTER

1 Introduction

1.1 Battery evolution

A power eater is a product or component whose power requirement exceeds the capacity of current battery technology. In the past, these "power eaters" have motivated the evolution of the battery as shown in Figure 1-1. For example, the shift from nickel metal hydride (NiMh) and nickel cadmium (NiCd) rechargeable batteries to current lithium-ion (Li-ion) rechargeable batteries occurred because "power eaters" like camcorders and notebook personal computers (PCs) consumed much more power than their previous counterparts. These power eaters first used the Li-ion battery, which then spurred the growth of cellular phones, digital cameras and personal digital assistants (PDAs). Mobile phones offering new features are the current power eaters, and fuel cells are currently the most plausible candidate to replace Li-ion rechargeable batteries.

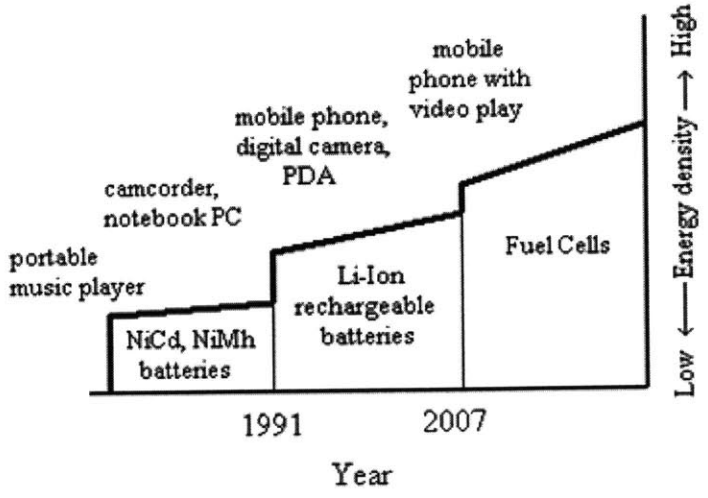

Figure 1-1 Power Eaters and Battery Evolution [1]

The current most commonly expanding features in mobile phones are miniature hard disk drives, wireless local area networks, and terrestrial digital broadcasting implemented in May 2005 in Korea and 2006 in Japan. These features drain large amounts of battery power, and at this rate, even the 10% annual capacity growth rate of Li-ion rechargeable batteries will not be sufficient to power cell phones with these new features for a reasonable length of time as shown in Figure 1-2. Thus, a new type of power source is necessary: the fuel cell [1].

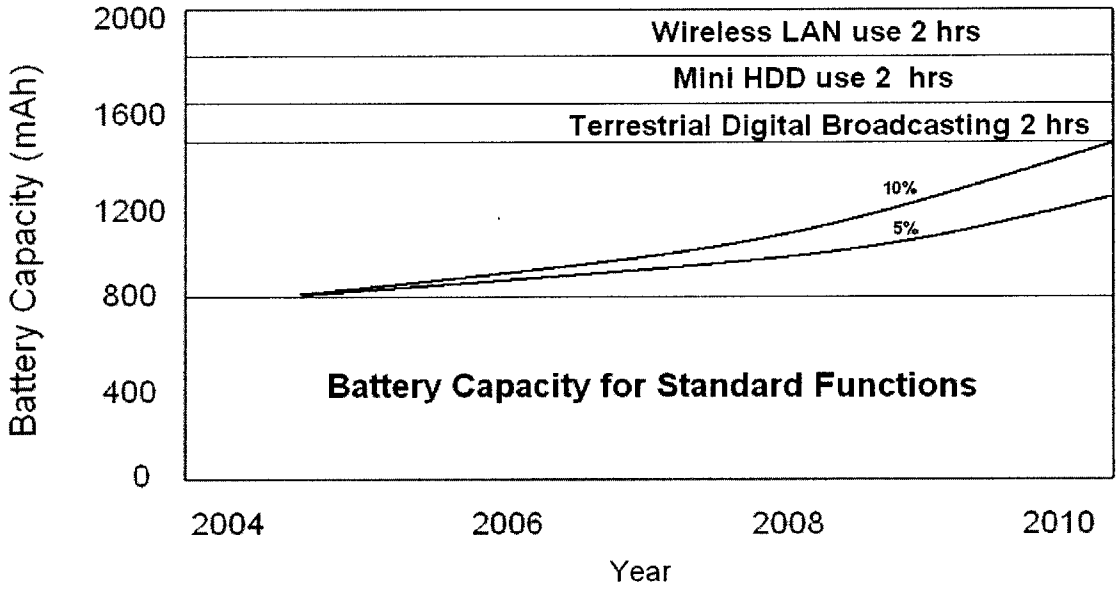

Figure 1-2 Battery Capacity of Li-ion Rechargeable Battery [1]

1.2 Current fuel cell research for personal mobile devices

Most mobile communications carriers have been doing fuel cell research for mobile devices for the past several years. The most widely developed fuel cells for mobile devices have been the direct methanol fuel cell (DMFC). Although, many have boasted in the past of impending commercialization of mobile devices powered by fuel cells, they have not yet been introduced to the market. Prototypes up to date have been

too big and bulky and more importantly have not been capable of providing enough power to justify commercialization [2].

Progress has been made, but there still exists many problems such as low power density and efficiency, miniaturization, ventilation of water and carbon dioxide, and cost that are preventing commercialization [3]. Currently, most companies have shifted their focus from mobile devices that are powered directly by fuel cells to fuel cell chargers that recharge the mobile devices when the battery power is low. These chargers are still a bit bulky, but some have claimed to provide enough power to recharge a mobile phone battery up to three times [2].

1.3 Objectives

If fuel cells are going to be adopted as the new power source for personal mobile devices, there are certain customer needs that must be met. The fuel cells must be comparable in price and size, which is on average $9cm^3$, to the current Li-ion batteries, while offering longer lasting power and a quicker charge time.

The objective of this research is to use an Axiomatic Design approach to investigate the key problems that limit DMFC efficiency in order to design and build a DMFC-battery hybrid system that can power a mobile electronic device. However, a hybrid involving a battery is quite complicated, and so the initial fuel cell design will be integrated with a capacitor to create a fuel cell – capacitor hybrid. To pursue this, three different areas for improvement in the context of one integrated unit were considered:

1) Increase the Performance of the fuel cell
2) Decrease the total volume of the fuel cell unit
3) Connect to a hybrid circuit

1.4 Organization of the thesis

This thesis concerns an integrated design approach for fuel cells for mobile devices. Chapter 2 provides background information on direct methanol fuel cells, the electrochemical reaction in these fuel cells, and begins honing in on two hurdles that prevent efficient fuel cell performance. Chapter 3 outlines the goals for the fuel cell design and describes the design process and choices. One of the most difficult parts of this research effort was to create the parts of the fuel cell. Thus, Chapter 4 presents a detailed documentation of the fabrication process of the fuel cell design from Chapter 3. Chapter 5 provides the results of the fuel cell performance experiments and discusses the results. Chapter 6 provides background on hybrid devices and presents the design of the hybrid circuitry for a fuel cell used in a mobile device. Finally, Chapter 7 summarizes the findings and suggests future work.

CHAPTER

2 Background

2.1 Direct methanol fuel cells

There are several types of fuel cells, but for mobile devices, the DMFC has been considered the most promising candidate. There are several reasons that the DMFC is a good choice as a fuel cell for mobile devices. Firstly, methanol is readily available and low in cost. Secondly, methanol has a very high net energy density of 18.9MJ/kg. In addition, using methanol directly as a liquid fuel eliminates the hydrogen storage problem, which is a huge barrier to commercialization in most other types of fuel cells. Thus, using methanol directly keeps the total size of the fuel cell small.

Figure 2-1 shows the three basic components of a DMFC.

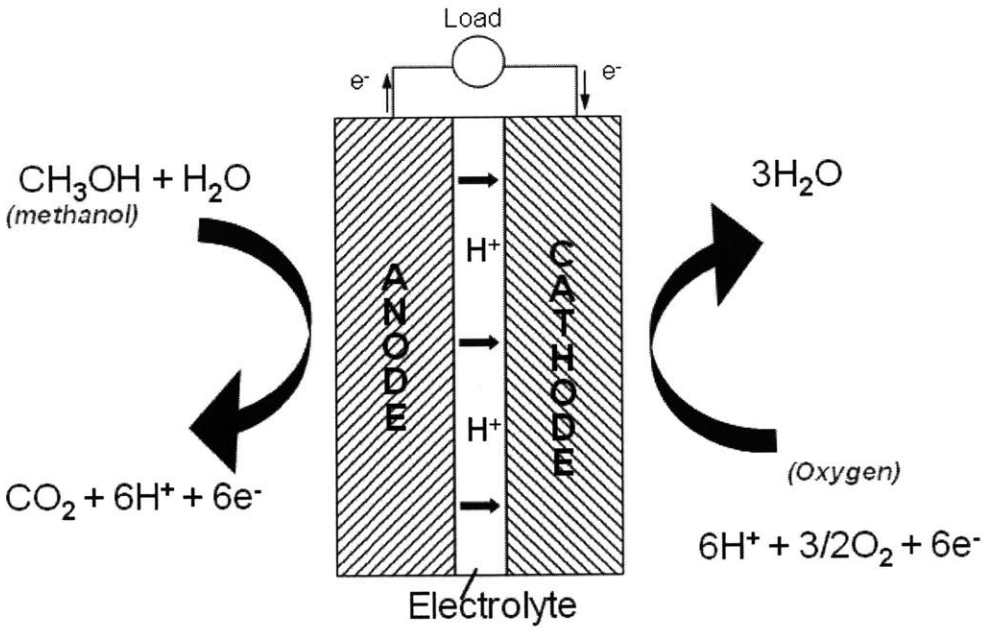

Figure 2-1: Schematic Diagram of Direct Methanol Fuel Cell

The anode is the negative post of the fuel cell. It conducts the electrons that are freed from the methanol/water mixture so that they can be used in an external circuit. The electrolyte is the proton exchange membrane (PEM). This specially treated material only conducts positively charged ions and blocks electrons so the protons from the anode pass through it to the cathode. The cathode is the positive post of the fuel cell, which conducts the electrons back from the external circuit to the catalyst, where they can recombine with the hydrogen ions and oxygen to form water. Catalysts are placed on both the anode and cathode sides to facilitate the reactions occurring at those locations [4].

For a DMFC, the overall reaction at the anode is:

$$CH_3OH + H_2O \rightarrow 6H^+ + 6e^- + CO_2 \qquad \textbf{2-1}$$

where CH_3OH is methanol, H_2O is water, H^+ is a proton, e^- is an electron, and CO_2 is carbon dioxide.

The overall reaction at the cathode is:

$$\frac{3}{2}O_2 + 6H^+ + 6e^- \rightarrow 3H_2O \qquad \textbf{2-2}$$

where O_2 is oxygen.

The overall reaction that takes place in a DMFC is:

$$CH_3OH + \frac{3}{2}O_2 \rightarrow 2H_2O + CO_2 \qquad \textbf{2-3}$$

2.2 Fuel cell electrochemistry

There are several important definitions and basic electrochemical principles that will aid in the understanding of fuel cells and their operation.

2.2.1 Open Circuit Voltage

The open circuit voltage (OCV) is the voltage measurement of a fuel cell when there are no losses. In a fuel cell, chemical energy is converted into electrical energy; the chemical energy that is converted is referred to as the Gibbs free energy. When all the Gibbs free energy is converted into electrical energy, there are no losses, and an OCV can be obtained.

In a fuel cell, electrical work is done by the movement of electrons. Two electrons pass around the external circuit for each hydrogen molecule that is used and for each water molecule that is produced. In the case of a DMFC, 6 electrons are passed via the external circuit for every hydrogen molecule that is extracted from the methanol. Electrical work, W, for a DMFC can be expressed as:

$$W = -6FE \qquad \textbf{2-4}$$

where F is the Faraday constant and E is the voltage of the fuel cell.

If the system has no losses, then the electrical work done is equal to the chemical energy, or Gibbs free energy, $\Delta \overline{g}_f$, that is released. Thus,

$$\Delta \overline{g}_f = -6F \cdot E$$
$$E = -\frac{\Delta \overline{g}_f}{6F} \qquad \text{2-5}$$

Equation 2-5 gives the theoretical open circuit voltage for a DMFC. The theoretical OCV for a DMFC is 1.21 volts. However, in practice, the actual measured OCV of a fuel cell, which can be easily measured using a multimeter, is always lower than the theoretical OCV and is closer to 0.7V for a DMFC. This is due to the irreversibilities of the fuel cell that is even apparent in smaller amounts when no current is drawn.

Overvoltage or overpotential is a term used by electrochemists to describe the voltage difference between the ideal and actual operating fuel cell voltage. There are four types of major losses that cause cell overvoltage in a DMFC: losses due to the ohmic resistance, kinetics, fuel crossover, and mass transport [4].

2.2.2 Ohmic Losses

Ohmic losses are caused by the electrical resistance of the electrodes and the resistance of ion flow in the electrolyte, although the former resistance is the main contributor for these losses. The voltage drop due to ohmic resistance, $\Delta V_{ohm,}$ can be modeled simply as:

$$\Delta V_{ohm} = i \cdot r \qquad \textbf{2-6}$$

where i is the current density given in units of mA/cm^2 and r is the area-specific resistance given in units of $k\Omega/cm^2$.

The area-specific resistance, r, can be calculated by:

$$r = t / \sigma \qquad \textbf{2-7}$$

where t is the electrolyte thickness and σ is the conductivity given in units of S/cm [5]. Given that the electrolyte Nafion 117 has a thickness of 0.18 mm and an approximate conductivity of 0.09 S/cm, the area-specific resistance is approximately 0.0002 $k\Omega/cm^2$ in the case of a DMFC with Nafion 117 as an electrolyte [6].

2.2.3 Activation losses

Activation loss is caused by the slowness of the kinetic reaction taking place at an electrode. Of the four losses, decrease in voltage efficiency due to activation loss accounts for the greatest efficiency loss, at 50% of the total losses. Especially in a direct methanol fuel cell, these losses occur both at the anode and cathode.

These losses were first experimentally observed by Tafel [4]. It was observed that overvoltages at the surface of the electrodes followed a similar pattern in various electrochemical methods. This pattern can be observed in a plot of the overvoltage vs. the natural logarithm of the current density, known as Tafel plots. The overvoltage by activation losses, ΔV_{act}, is given by Equation 2-8, which is also known as the Tafel equation, where A is a constant and i_0 is called the exchange density.

$$\Delta V_{act} = A \cdot \ln\left(\frac{i}{i_o}\right) \quad \text{2-8}$$

The constant A for a DMFC is given by:

$$A = \frac{RT}{6\alpha F} \quad \text{2-9}$$

in unit of volt where R is the molar gas constant, T is the temperature, and constant α is the charge transfer coefficient. The charge transfer coefficient is dependent on the material of the electrode and the reaction involved and is within a range from 0 to 1. The hydrogen electrode usually has a value of about 0.5 and the oxygen electrode is between 0.1 and 0.5. Given the small range of both of these values, this constant plays a small role in determining the value of A or the voltage change.

In fact, it is the exchange current density that has the greatest impact on the activation loss. The exchange current density is a quantity that measures the current from the flow or "exchange" of electrons that is occurring from and to the electrolyte. The higher the exchange current density, the more active the surface of the electrode is. Thus, a high current density is desired and necessary for an efficient fuel cell [4].

2.2.4 Losses due to fuel crossover

Currently, the PEM is the only electrolyte that is a potential option for a DMFC membrane. However, because methanol mixes well with water, methanol tends to cross over through the membrane to the cathode side of the fuel cell. This is a waste of fuel and it also causes reduction in the cell voltage because it slows down or blocks reactions happening at the cathode. Losses due to fuel crossover are difficult to distinguish and

measure from other losses, but with low-temperature fuel cells, the loss due to fuel crossover is at least 0.2 volts [4].

2.2.5 Losses due to mass transport

When a reaction occurs at the cathode, the amount of oxygen, supplied in the form of air, decreases as the oxygen is extracted. Similarly at the anode, there will be a decrease in concentration of the fuel where the reaction occurs. The change in concentration is dependant on the current being drawn from the cell, how well the product is distributed, and how fast the product is replenished. In both cases, the change in mass transport will cause a voltage drop in the fuel cell.

Unfortunately, at the current moment, there is no analytical model for the losses due to this phenomenon. However, an empirical solution discovered by Kim *et al.* has been widely accepted and used by the fuel cell community. Equation 2-10 shows the change in voltage due to mass transport , ΔV_{trans}, given that m and n are chosen correctly.

$$\Delta V_{trans} = m \cdot \exp(ni) \qquad \textbf{2-10}$$

where m and n are constants that can be obtained by a non-linear regression analysis and have the units of volt and reciprocal of current density, respectively. A typical value of m is 3×10^{-5} V and a typical value of n is 8×10^{-3} cm^2/mA [7].

2.2.6 Polarization Curves

The various irreversibilities discussed in the previous sections can be combined into Equation 2-11 to show the net effect on the fuel cell voltage, V.

$$V = E_{ocv} - \Delta V_{ohm} - \Delta V_{act} - \Delta V_{trans}$$

$$V = E_{ocv} - ir - A\ln\left(\frac{i_f + i_n}{i_0}\right) + m \cdot \exp(ni) \qquad \text{2-11}$$

where E_{ocv} is the OCV and i_f is the current density due to fuel crossover and i_n is internal current density.

The combined effects of these losses on the performance of a fuel cell can be measured and seen by polarization curves or voltage vs. current density plots. This can easily be plotted by varying the voltage from the OCV to zero and measuring the current. The current density can be calculated by dividing the current by the catalyst area. A typical voltage vs. current density plot can be seen in Figure 2-2.

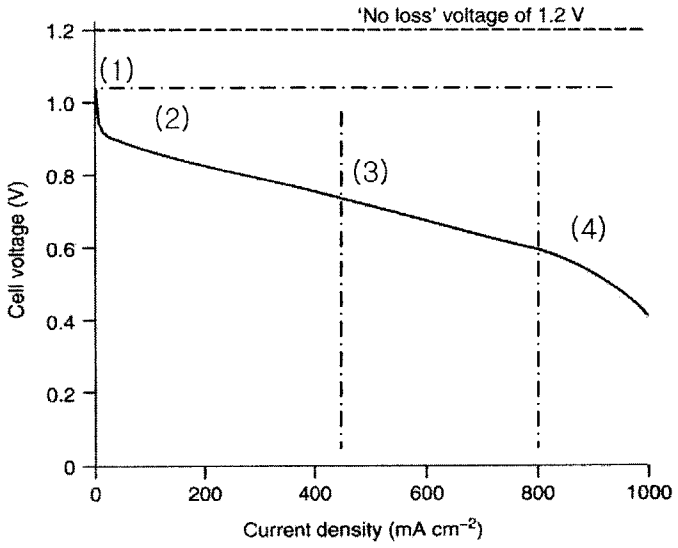

Figure 2-2 Voltage vs. Current Density Plot: Losses due to (1) fuel cross over, (2) activation, (3) ohmic resistance, (4) mass transport [4]

In Figure 2-2, the loss due to fuel cross over is shown by the gap between the theoretical 'no loss' voltage and the OCV of the actual fuel cell. The overpotential due to activation losses is observed at low current densities and is non-linear. The voltage loss due to ohmic resistance is the most straight and is fairly linear to current density.

Mass transport or concentration loss has the greatest effect in high current density regions.

Another way performance can be measured is by voltage vs. power density plots. This can be plotted by taking the current density values from the voltage vs. current density plot and multiplying it by the associated voltage [4].

2.3 Membrane electrode assembly

The two electrodes, cathode and anode, and the electrolyte make up the membrane electrode assembly (MEA). The MEA is the most important component in a fuel cell. Its performance has a strong impact on stack performance, as well as durability, and cost; the higher power density generated per unit area, the less hardware needed, which makes stacks smaller, lighter, and also less expensive [8]. There are two main issues in the MEA that will be addressed in the following two sections: flooding at the cathode and methanol crossover.

2.3.1 Flooding at the cathode

In the DMFC cathode, one reason for activation loss is due to the presence of large amounts of water, which causes flooding. The presence of water at the cathode prevents the oxygen from reacting with the cathode catalysts, thus slowing the reaction and resulting in a voltage loss. Large amounts of water are present at the cathode because for every mole of methanol, about 2.5 x 6 water moles are transported to the cathode, assuming that the electro-osmotic drag coefficient of water is equal to 2.5 per proton [9]. Plus, an additional three moles of water are produced at the cathode by consuming the six protons created from the methanol oxidation reaction at the anode, which amounts to a total of 18 moles of water at the cathode.

Traditionally, a high gas flow rate at the cathode is used to prevent flooding. Devices such as a pump or condenser have been used to recycle the water from the cathode to the anode. However, these changes require higher power consumption and additional parts, which prevent the fuel cell from being small enough to be used in personal mobile devices, such as cellular phones.

G.Q. Lu et al. modeled the total rate of water arrival and production in the cathode, j_{H_2O}, as:

$$j_{H_2O} = \left(\alpha_{H_2O} + \frac{1}{2}\right)\frac{1}{F} \qquad \textbf{2-12}$$

where α_{H_2O} is the net water transport coefficient, which is a combined result of electro-osmotic drag, diffusion, and hydraulic permeation through the membrane. In thicker membranes used in DMFCs, such as that of Nafion 117, α_{H_2O} approaches the osmotic drag coefficient as the other two modes of water transportation have less of an effect [10]. Equation 2-12 shows that in order to decrease flooding, a low value of α_{H_2O} is desired. A low value for α_{H_2O} can be achieved by increasing the hydraulic pressure in the cathode. Peled *et al.* achieved this by using a hydrophobic gas diffusion layer (GDL). This pressure difference promotes low water back-flow and prevents flooding in the cathode. The hydraulic pressure, p_h, can be expressed as the combination of the pressure difference between the two sides of the electrodes, Δp_g, and the pressure required to fill a hydrophobic porous area with water, Δp_c. The relation is shown as:

$$p_h = \Delta p_c + \Delta p_g \qquad \text{2-13}$$

When a fuel cell is working at atmospheric pressure, Δp_g is equal to zero. Thus, p_h can be expressed as:

$$p_h = p_c = 2\sigma_s \frac{\cos\theta_c}{r_c} \qquad \text{2-14}$$

where σ_s is the surface tension, θ_c is the contact angle between the water and the surface, which is greater than 90° for a hydrophobic GDL, and r_c is the typical pore radius of the GDL as seen in Figure 2-3.

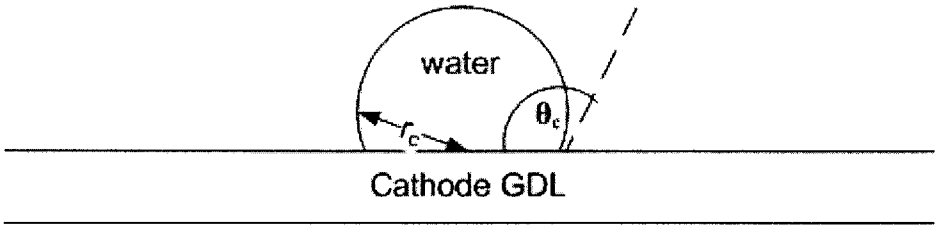

Figure 2-3 Water drop on Hydrophobic GDL

Increasing the hydrophobicity will increase the hydraulic pressure difference, which will lead to a lower α_{H_2O}. However, when $p_h > 2\sigma_s \cos\theta / r_c$, the hydraulic pressure is high enough to push the water through the pores of the GDL and to the outside layer of the cathode. Thus, p_h should be less than $2\sigma_s \cos\theta / r_c$ in order for the GDL to prevent the water from exiting and blocking oxygen reduction reaction sites at the cathode. This indicates that there is an optimum hydrophobicity and Equation 2-14 shows that the hydraulic pressure can be changed by the controlling contact angle and the pore radius of the GDL [11]. Lu et. al has suggested adding an additional layer to the GDL referred to as the microporous layer (MPL) to control the contact angle and pore radius. Similarly,

others have used a microporous coating or layer to control the hydrophobicity, either directly on the GDL or as an additional part [10, 11]. For the remainder of this document, the microporous coating will be referred to as the MPL.

2.3.2 Methanol Crossover

The issue of fuel crossover was previously discussed in Section 2.2.4. There are several standard techniques that have been used to decrease methanol crossover. The first is increasing activity at the anode catalyst by using more catalysts in hopes for a faster reaction and therefore a quicker consumption of the methanol before it can cross over. But adding more catalysts is costly and is not entirely effective. Another method to prevent methanol crossover is controlling the fuel feed to the anode. This would be done via a sensor with feedback system that would control the water/methanol mixture. This complicates the system greatly and creates a bigger package, which is an unfavorable characteristic in mobile devices. Another option is to change the composition of the membrane itself to block methanol from crossing over [8].

A good DMFC membrane would have two qualities: good proton conductance, which Nafion is best for, and an effective methanol barrier, which Nafion does not provide. Shao *et al.* defined a membrane's tendency to conduct protons versus methanol as the term, β. β is expressed as:

$$\beta = \frac{i/\Delta\phi}{j_{CH_3OH}/\Delta C} \qquad \textbf{2-15}$$

where j_{CH_3OH} is the methanol flux in the membrane, Δφ is the electrostatic potential difference and ΔC is the methanol concentration difference. Relative selectivity, α_R, was

used to compare the selectivity of a modified membrane to that of the unmodified Nafion membrane as:

$$\alpha_R = \frac{\beta_m}{\beta_N} \qquad \textbf{2-16}$$

where β_m is the selectivity of the modified membrane and β_N is the selectivity of the unmodified Nafion membrane. Shao *et al.* used a composite Nafion/Polyvinyl Alcohol (PVA) membrane made from a casting solution, which was followed by cross-linking to improve the mechanical strength of the treated membrane. It was found that PVA is good for methanol selectivity; however, it is bad for proton conductance and causes a significant resistance that reduces the overall voltage. Thus, a final sulfonation treatment was added to improve the membrane conductance. In addition, a Nafion/PVA treated membrane was sandwiched between two untreated Nafion membranes for slightly better performance [12].

Others such as Wang *et al.* and Kang *et al.* have used variations of PVA and other polymer blends such as poly styrene sulfonic acid (PSSA) to produce similar results of decreased methanol permeability and improved DMFC performance [13, 14].

CHAPTER

3 Fuel cell design

3.1 Functional design of the fuel cell for mobile devices

An Axiomatic approach to design was adopted to investigate the key problems that limit DMFC efficiency in order to design and build a DMFC that is an improvement on a current design. In Axiomatic design, there are four domains: customer, functional, physical, and process domain. The focus of this section will be on the design of the product, which depends on the mapping for the functional domain to the physical domain. In order to do this, there are design parameters that must fulfill functional requirements. Functional requirements (FRs) are defined as "the minimum set of independent requirements that completely characterize the functional needs of the product." It is essential that the functional requirements are independent as stated in the definition. Design parameters (DPs) are defined as "the key physical variables in the physical domain that characterize the design that satisfies the specified FRs." It is important to note that although ideally these would be independent physical variables, multiple DPs could be satisfied with a single design part [15].

3.1.1 Functional requirements

Top level FR/DP pairs outline the problem statement for this research. As similarly outlined in the objectives, this design can be decomposed into the following three top level functional requirements:

- FR1: Increase fuel cell performance

- FR2: Decrease fuel cell volume
- FR3: Connect to a hybrid circuit.

As described above, each functional requirement will have a corresponding design parameter or solution.

3.1.2 Design parameters

Ideally, each design parameter would meet the independent requirements set forth by the functional requirements. Here are the design parameters:

- DP1: Membrane Electrode Assembly
- DP2: Passive Air Cathode Structure
- DP3: Fuel Cell Capacitor Hybrid Circuitry

The first two design parameters will be addressed in this chapter. The third design parameter will be discussed in Chapter 6.

3.1.3 Decomposition of the MEA

The MEA has three basic FRs:

- FR11: Oxidation of methanol
- FR12: Reduction of oxygen
- FR13: Move protons from the anode to the cathode

The corresponding DPs are as follows:

- DP11: Methanol and water reaction
- DP12: Oxygen, proton, and electron reaction
- DP13: Protonic conductive membrane

There are many inefficiencies in a DMFC. One of the inefficiencies occurs at the cathode where oxygen reduction takes place. In order for this reaction to take place, oxygen, protons, and electrons must come together. However, in a DMFC, two prominent problems, flooding and methanol crossover, slow down this reaction. Flooding at the cathode causes water molecules to cover the cathode GDL and prevent oxygen from reacting with the protons and cathode catalyst. Similarly, methanol crossover blocks the protons from reacting with the oxygen and thus slows down the oxygen reduction at the cathode. In order to prevent methanol crossover, membranes other than the Nafion membrane have been tested. However, this change tends to negatively affect FR13, moving protons from the anode to the cathode. Thus, it is important to discover a solution that decreases the methanol crossover while unaffecting the protonic conductivity of the membrane.

3.1.4 Decomposition of the passive air cathode structure

There are three FRs that is to be achieved in a passive air cathode structure.

- FR21: Decrease volume
- FR22: Allow oxygen to pass through to the cathode catalyst
- FR33: Move electrons from the cathode to the anode

The corresponding DPs have been chosen:

- DP21: Eliminate pump
- DP22: Air-breathability
- DP23: Conductivity of the cathode

These design choices and implementation are further described in Section 3.3.

3.2 MEA modifications

In order to increase the fuel cell performance, two modifications have been pursued for the fuel cell for mobile devices: the addition of a MPL at the cathode and the replacement of Nafion membrane with PVA/Nafion membrane.

3.2.1 Microporous Layer

Based on a literature survey, experiments done by Lu *et al.* were chosen, due to their well documented process, to create a MPL on a GDL made of carbon paper that would prevent flooding at the cathode. However, the paper failed to include the exact amount of some of the elements that are used to create the MPL paste. Thus, a prefabricated MEA with a GDL that had an MPL was purchased and used as the standard to compare the modified MEAs. An MEA with a cathode GDL made of carbon cloth with ELAT, which serves as an MPL, was purchased from the Fuel Cell Store. ELAT is a trademark material from E-TEK. It is a carbon cloth that maximizes gas transport to the cathode catalyst while allowing water and unwanted reactants to move away from the area [16]. In addition, a carbon paper GDL with an MPL, similar to the MPL produced by Lu, was purchased from SGL Carbon Group.

3.2.2 Nafion/PVA membrane

As previously discussed in Section 2.3.2, variations of PVA, PSSA, and other polymer blends have been used in composite with Nafion in order to decrease methanol crossover in DMFCs. Based on additional literature survey, reported findings, and the availability of detailed documentation, it was decided to follow the experiments performed by Shao *et al.* to create a membrane that decreases methanol crossover.

According to Shao, many acid-base blend membranes have produced good performance data but have not had long-term reliability analysis. In addition, other membrane blends have compromised mechanical strength and/or decreased proton conductivity. Shao created a Nafion 117/PVA membrane from a casting solution of weight ratio 1:1 of Nafion and PVA. In addition, in order to make sure that the mechanical strength was not compromised, a cross-linking solution was used to enhance the mechanical strength of the membrane. To prevent loss in proton conductivity, a sulfonation process was also used.

Further testing showed that the number of immersion treatments in the casting solution changed the membrane thickness and affected the relative selectivity and the resistance of the membrane. Three immersion treatments showed the best results. In addition, a thinner Nafion 112 was treated and sandwiched between two non-treated Nafion 112s in order to decrease the interfacial resistance between the PVA film and catalyst caused by poor adherence between these two layers. This was compared to the performance of three non-treated Nafion membranes and showed better selectivity, but an increase in resistance. Based on Shao's data, it appears that there is a very small difference in performance between the Nafion 117/PVA membrane immersed three times and the Nafion 112/ PVA membrane sandwiched between two untreated membranes. The slight tradeoff is that the former had better methanol selectivity whereas the latter had lower resistance. Based on the trivial difference, it was decided that the Nafion 117/PVA membrane immersed three times would be used as the membrane for this fuel cell because it would be easier to fabricate [12].

3.3 Passive Air Cathode

3.3.1 Mobile device fuel cell system packaging

With the shift from 2G to 3G mobile phone technologies, cellular phones have become more complicated and costly in the recent years. On top of this, recent advancements in 3G phones such as Universal Mobile Telecommunications System communications, which allow faster processing speeds for new functions like terrestrial digital broadcasting, only add to the complication and cost. Thus, cellular phone and other mobile device manufacturers are faced with the challenges of not only keeping the cost low, but also keeping the overall package volume down on these devices that carry the new emerging technology; consumers expectations of device performance are rising, while they expect the device size to stay the same, or decrease [17].

There are several factors that hinder commercialization of a mobile device that runs off a fuel cell and size is one of them. In addition to the several cells that need to put together to form a stack for increased voltage output, fuel cells also often need pumps on the anode side, to pump fuel, methanol in the case of DMFCs, and on the cathode side, oxygen. When the reactants are pumped with higher pressure, there is an increased efficiency [18]. However, the pump systems take up a lot of space.

Because there is no fixed orientation for mobile phones, in a DMFC, the liquid fuel has to be pumped at the anode side; yet, there is a possibility to take out the pump at the cathode side and have a passive air breathing fuel cell. Instead of having a thick plate made of graphite or some other material with a flow pattern on the cathode side, a mesh made of conductive material with passive air flow can be used. However, there is a tradeoff; with only one side being pressurized, there will be a decrease in performance

compared to a fuel cell using pressurized oxygen. On the other hand, there is a decrease in the overall volume, which is important in mobile devices. Even if a fuel cell were to provide sufficient power, it cannot be much larger than the power sources that are used today.

3.3.2 Design of cathode mesh

There are two requirements that must be fulfilled for the cathode electrode: it must allow ambient air to have access to the catalyst on the MEA and it must be conductive [8]. In addition to ambient air access, for a fuel cell for mobile devices, minimizing the size is important. Given the requirements, a metallic mesh was considered to be the best design option.

Figure 3-1 shows the front view of the cathode side of the fuel cell with a mesh design.

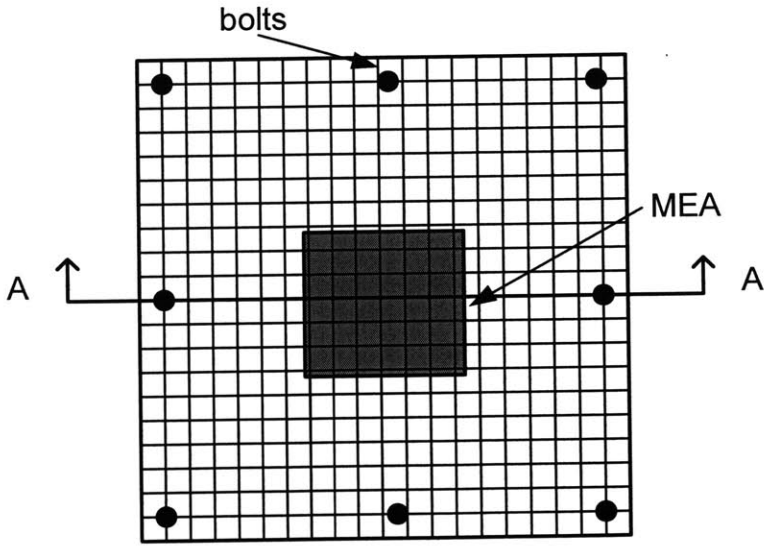

Figure 3-1 Cathode front view with mesh, first design

Figure 3-2 shows the cross-sectional schematic of the fuel cell with the cathode mesh, Section A-A, in comparison to a standard fuel cell.

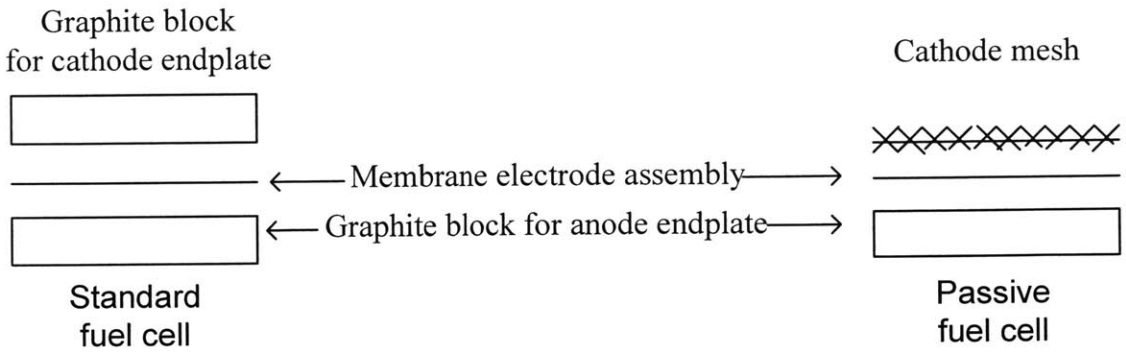

Figure 3-2 Cross-sectional schematic of standard vs. passive fuel cell design (Section A-A from Figure 3-1)

This was the first design of the cathode mesh. At the first run of experiments, it was discovered that this design would not be sufficient. Due to the flimsiness of the thin wire mesh, the mesh did not provide enough pressure to make good contact with the MEA, causing insufficient electrical conductance. In addition, the inadequate pressure from the mesh on the MEA caused the leaking of methanol on the anode side before it was able to react at the MEA and damaged the MEA as seen in Figure 3-3.

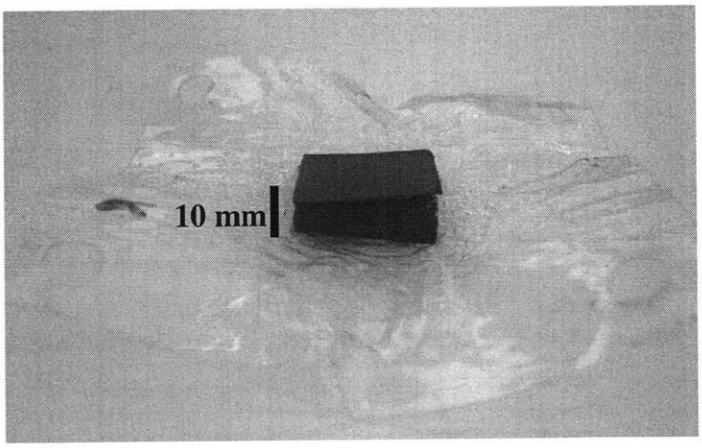

Figure 3-3 Damaged MEA

A second generation design was created to provide reinforcement to the cathode mesh. This was done by taking a thin metal sheet of 0.635-mm thickness and cutting an

opening for the MEA. This plate was then placed in front of the original cathode mesh as seen in Figure 3-4.

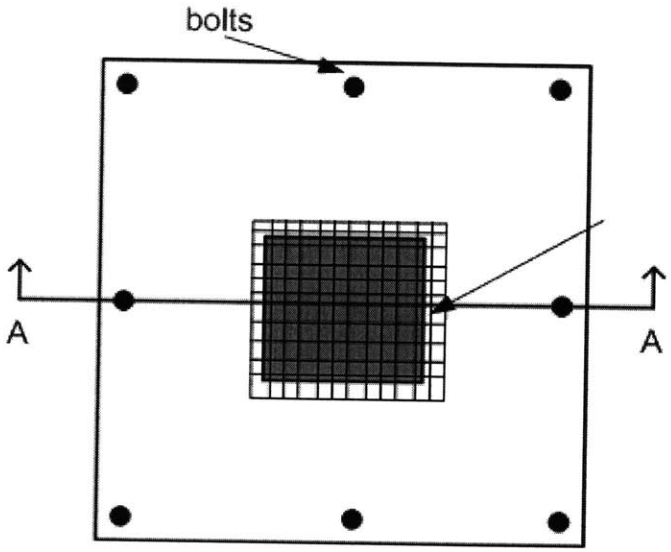

Figure 3-4 Cathode front view with mesh, second design

Section A-A of the second generation fuel cell with a mesh design can be seen in Figure 3-5.

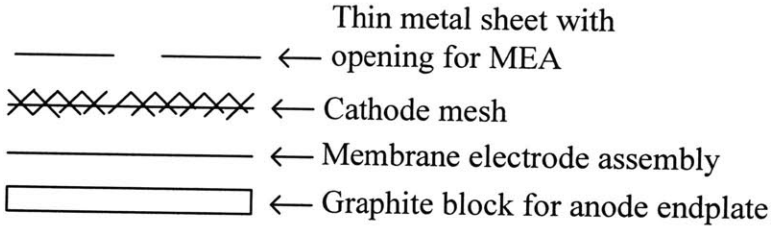

Figure 3-5 Section A-A of fuel cell with cathode mesh, second design

The next run of experiments was successful until the flow rate was increased. Because of the malleability of the thin metal sheet, it was discovered that it did not provide even pressure on the MEA and again, caused the leaking of methanol on the anode side before it was able to react at the MEA.

A third generation design was created in which the thin metal sheet was replaced with a thicker metal plate, 4.762-mm thick. This plate was placed in front of the original

cathode mesh like the thin sheet metal in Figure 3-4. Although the thicker metal plate takes up more volume than solely using the mesh, it still reduces the overall size of the original fuel cell.

Since they generally have good conductivity, various metals were considered for the mesh. Lu *et al.*, Jaouen *et al.*, and Shimizu *et al.*, have used stainless steel in their passive air cathode fuel cell design [10, 19, 20]. Stainless steel has low conductivity, but it is corrosion resistant. For Jaouen and Shimizu, an increase in fuel cell performance was noted by coating the stainless steel with gold for improved conductivity. For this design, copper was chosen due to its high conductivity and availability. Although copper is not corrosion resistant, a coating of gold could eliminate this problem. For this research, a plain copper mesh was used. For the second design with the thin metal sheet, copper was also used. For the final design, aluminum was used for the metal plate. However, the fact that aluminum was used instead of copper did not make a difference in the current and voltage reading because the cathode side readings were taken directly from the copper mesh.

In regards to conductivity, various mesh sizes were considered. However, after taking resistance measurements of various mesh sizes, it was discovered that the difference in calculated conductivity of the wire meshes was very small as seen in Table 3-1.

Table 3-1 Various wire mesh resistance and conductivity

Wire mesh	Resistance (Ω)	Conductivity (S/m)
Square size: 1.32 mm, Wire diameter: 0.28 mm	1.0	10.5
Square size: 5.16 mm, Wire diameter: 1.19 mm	1.1	9.6
Square size: 11.10 mm, Wire diameter: 1.60 mm	1.0	10.5

In regards to the area needed for the oxygen reduction to occur, various mesh sizes were also considered. Based on availability and cost, a woven medium copper mesh with a percentage of open area of 67.9% and with openings of 1.74 mm^2 was used.

At the third attempt to run experiments it was discovered that this design would still be insufficient. The fuel cell OCV remained zero. This suggested that somewhere in the fuel cell, the circuit was shorting. It was discovered that due to the frailty of the thin copper mesh, as seen in Figure 3-6, small pieces of the copper wires were coming in contact with the edges of the conductive graphite block on the anode side of the fuel cell.

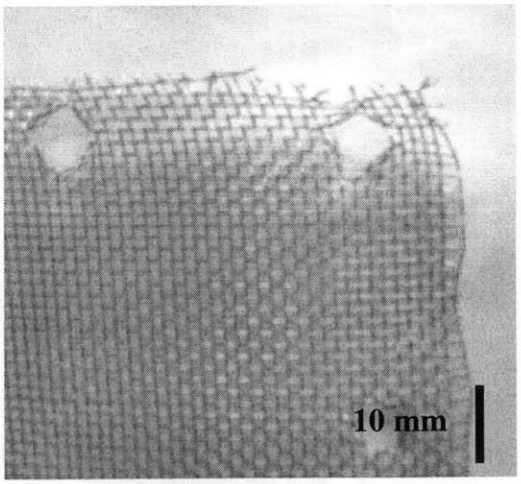

Figure 3-6 Frazzeled edges of copper mesh

These points of contact occurred at the edges and also at the metal bolts that kept the fuel cell together. Two changes were made to fix this problem. Firstly, black

electrical tape was used to reinforce the frazzled edges of the copper mesh around the outside of the fuel cell along with the edges near the bolts as seen in Figure 3-7.

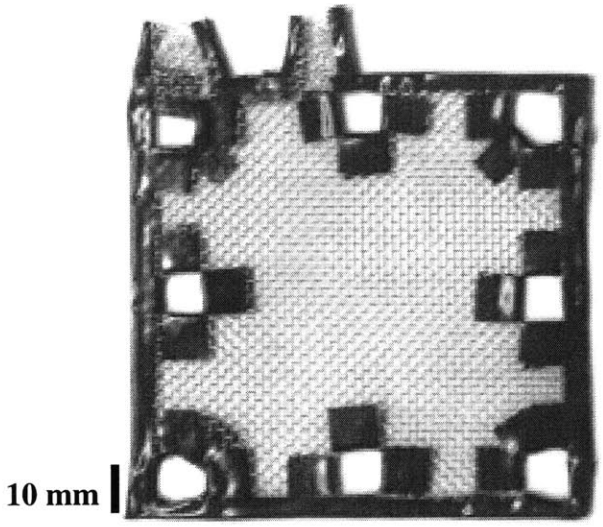

Figure 3-7 Modified copper mesh

Secondly, plastic tubes were inserted around the bolts on both the anode and cathode side to prevent contact between the metal nuts and bolts and the conductive graphite from the anode side and copper from the cathode side in Figure 3-8.

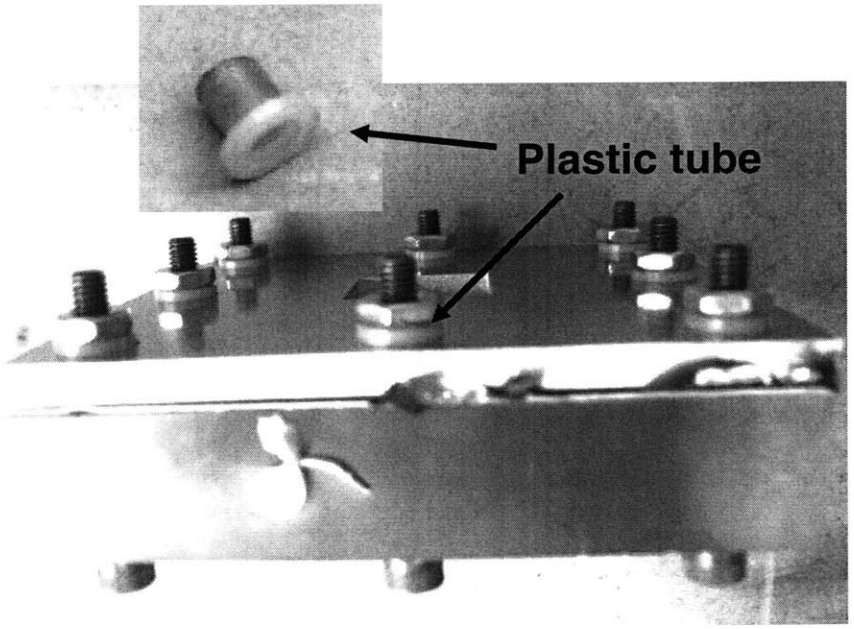

Figure 3-8 Plastic tubes to prevent shorting

3.3.3 Methanol concentration for passive fuel cell

In the DMFC anode, for each mole of methanol, 1 mole of water is consumed and 15 moles of water is transported to the cathode. This corresponds to approximately 3 molarity (M). Thus, water must be replenished at the anode if methanol concentrations greater than 3M are used [10]. Higher concentration of methanol reduces the volume of stored methanol in an application. However, if water needed to be replenished at the anode, this would require a condenser at the cathode and an additional pump to transport the water from the cathode to the anode. The addition of these components is highly undesirable when trying to keep the overall size of the fuel cell small. Therefore, 3M methanol was used as a standard methanol concentration when running experiments in order to prevent the need to re-supply water to the anode side and ultimately keep the size of the fuel cell small.

CHAPTER

4 Fuel cell fabrication and test setup

4.1 Membrane electrode assembly modifications

One of the important aspects of this research is documenting the procedure of creating fuel cell components. A widely used and what appeared to be well documented procedure was used to create the MEA. However, modifications had to be made to these standard procedures and additional notes were recorded for more detailed documentation.

4.1.1 MEA manufacturing procedure

There are two main ways that an MEA is manufactured. The first is often referred to as the separate electrode method, in which the catalysts are fixed to a porous and conductive material such as carbon paper or carbon cloth. The anode and cathode electrodes are respectively fixed to each side of the membrane [8].

The second, often called the decal method was described by Wilson and Gottesfeld. This was the method chosen to create the MEA. The procedures are as follows. Nafion 5% solution and Pt-Ru or Pt-Vulcan XC72 were mixed for the anode and cathode side, respectively. Then water and glycerol were added and mixed and ultrasound extensively to create an ink. The weight ratios of the compounds can be seen in Table 4-1.

Table 4-1 Weight ratio of catalyst ink compounds

compounds	dry weight ratio
Pt:Ru	1:1
Pt:Vulcan XC72	60:40
Nafion 5% solution: catalyst	1:3
Catalyst:water:glycerol	1:5:20

Next, a clean Teflon blank film, the size of 4cm x 4cm, was coated with a thin layer of fluorocarbon spray, and the catalyst ink was painted on a pre-marked area of $5cm^2$, centered on the blank film, for both the anode and cathode with their respective inks. The films were baked in a convection oven at 135° C. Once the films were dry, the anode film, membrane, and cathode film were hot-pressed together. This was done by setting the press temperature initially at 100° C while a light load was applied. Then the press temperature was increased to 125° C. It was then pressed at 80atm for 90 seconds and removed from the press for cooling. Finally, the Teflon blank films were peeled from membrane. Figure 4-1 shows the primary series of steps taken to create the thin film catalyst layer bonded onto the membrane [21].

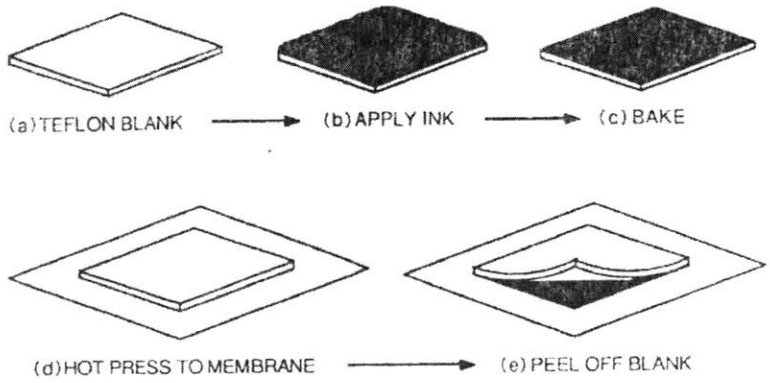

Figure 4-1 Decal method [21]

4.1.2 Thin film catalyst layer

The procedure in Section 4.1.1 was followed to create the MEA. After creating the cathode catalyst ink and preparing the Teflon blank, the ink was painted onto the Teflon blank. Figure 4-2 shows the first trial of the Teflon blank with Pt/Vulcan XC72 catalyst. The first trial shows an uneven blotchiness in the paint job and a curling deformity of the Teflon blank.

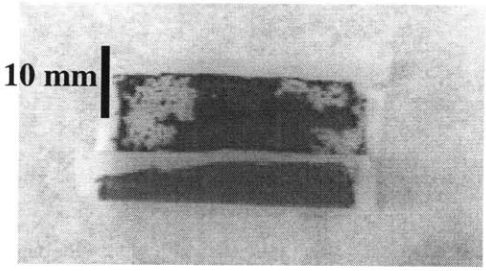

Figure 4-2 First trial of cathode catalyst painted onto a Teflon blank.

After several trials, it was observed that the fluorocarbon was unevenly sprayed onto the Teflon blank, and in general, there was a lack of fluorocarbon spray on the Teflon blank. A liberal amount of fluorocarbon spray on the Teflon blank shows a much more even painting of the catalyst layer in Figure 4-3. In addition, after spraying the first layer of the fluorocarbon, to ensure even coating, a second, and sometimes third, layer was sprayed after the first layer was completely dried. An even coating of the fluorocarbon spray could be visibly confirmed by an even white frosted layer on the Teflon blank.

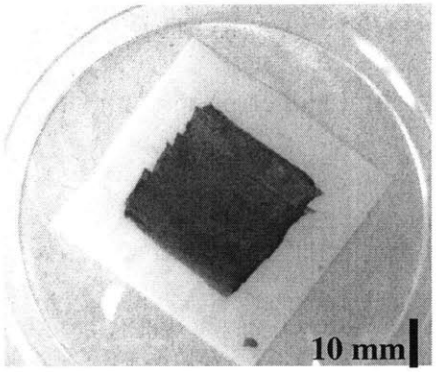

Figure 4-3 Successful cathode catalyst painted onto Teflon blank

The anode catalyst was created with more difficulty. Initially, the results were similar to that of Figure 4-2. Thus, a greater amount of fluorocarbon was sprayed and several layers were coated onto the Teflon blank. However, this still proved to be unsuccessful. After additional research, it was discovered that the different makeup of the anode catalyst ink that does not include carbon, unlike the cathode catalyst ink, caused the ink to be too thin. Thus, the water content was decreased so that when added to the Pt/Ru catalyst, it would be barely enough to cover it. This change allowed the anode catalyst ink to be successfully painted onto the Teflon blank. However, when put into the oven, the catalyst ink would burn up as seen in Figure 4-4.

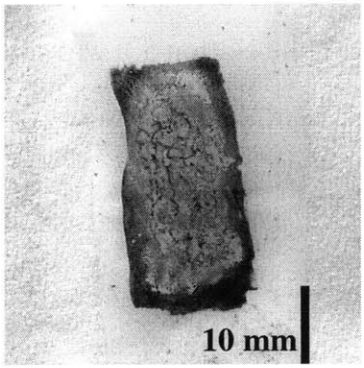

Figure 4-4 Burnt anode catalyst ink

Further research determined that Nafion contact with dry catalyst could be a cause of the burning. In addition, the fact that the water content was decreased, but the Nafion

content was left the same, could have been a contributing factor to the burning of the anode catalyst ink. After some trial and error, an optimal new ratio was determined for the mixing of the anode catalyst ink.

It is suggested that the Nafion 5% solution and Pt-Ru weight ratio and Pt-Ru to water and glycerol weight ratio is altered as shown in Table 4-2 for the anode catalyst ink.

Table 4-2 Modified weight ratio of anode catalyst ink compounds

compounds	dry weight ratio
Pt:Ru	1:1
Pt:Vulcan XC72	60:40
Nafion 5% solution: catalyst	1:40
Catalyst:water:glycerol	1:1:1.25

Furthermore, rather than mixing the Nafion 5% solution and Pt-Ru first, then adding the water and glycerol later, it is suggested that the water be added to the catalyst first. Once the catalyst was thoroughly wetted, the Nafion 5% was added along with the glycerol. This prevented any chances of the Nafion burning the catalyst.

A lower baking temperature of 70°C was used. In addition, the samples were checked periodically every 30 minutes to prevent over-baking. After these changes were made, a successful thin film catalyst layer was created similar to that of Figure 4-3.

The catalyst loading can be calculated by measuring the Teflon blank after the fluorocarbon spray and then again after the Teflon has the catalyst painted and baked in the oven. The difference in mass is the catalyst loading for the electrode. Depending on

the catalyst used, the percent of Pt on Carbon should be factored when calculating the catalyst loading.

4.1.3 Hot-pressing the MEA

Once the thin film catalyst layers for both the cathode and anode were successfully painted and dried onto the Teflon blank, continuing the procedure for MEA fabrication described in Section 4.1.1, the thin film catalyst layers were used to sandwich a Nafion 117 membrane. The first several runs created unsuccessful parts. The catalyst was not fully adhering to the membrane when the Teflon blanks were peeled off as seen in Figure 4-5.

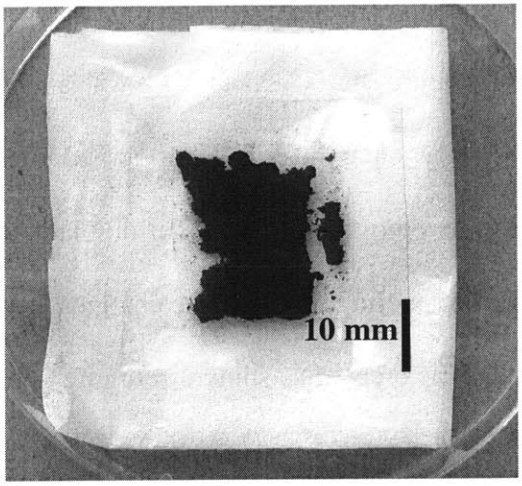

Figure 4-5 Unsuccessful catalyst adherence to membrane

After running several experiments, it was noticed that the catalyst was repeatedly not adhering in the same location on both sides of the membrane. It was thus suspected that it was not a problem with the painting technique but possibly the inaccuracy of the planarity of the hot press that was being used. After more tests, this was verified as the cause of the problem. Small metal plates, made of copper for good conductivity, the size of 38.1mm x 38.1mm x 0.8.76mm, and a 1-mm thick polymethyl-methacrylate (PMMA)

with a diameter of 30 mm were inserted on both sides of the MEA as shown in Figure 4-6.

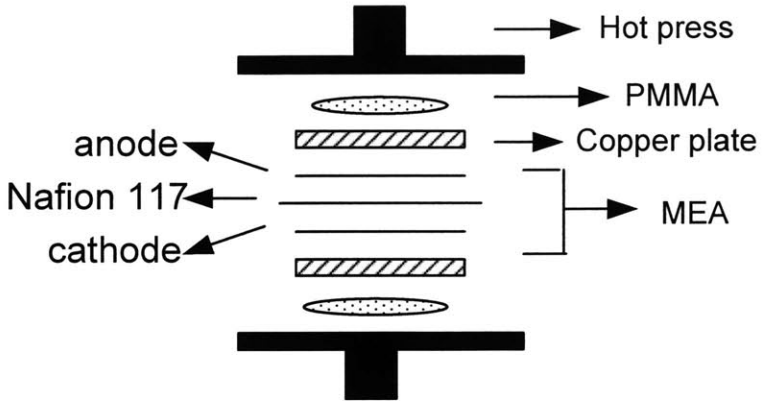

Figure 4-6 MEA fabrication setup

Because PMMA is a thermoplastic, it can be deformed once the temperature is greater than its glass transition temperature of 100°C. Thus, it was able to makeup for the non-planarity of the hot press. Lastly, once the MEA was cooled after being taken out of the hot press, a flat spatula was moved over the entire Teflon blank on both sides for additional reinforcement before peeling. With these changes, a successful MEA with Nafion 117 as the membrane was created as shown in Figure 4-7.

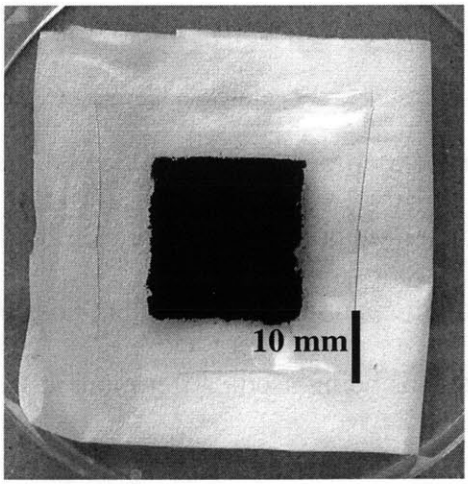

Figure 4-7 Successful MEA

4.1.4 PVA/Nafion Membrane

As discussed in Section 3.2.2, Shao created a Nafion 117/PVA composite membrane to decrease methanol crossover. The procedure from Shao was followed to add a Nafion/PVA composite layer on the membrane. First a casting solution of10wt% PVA water solution and 5% Nafion solution of 1:1 dry weight ratio was created. The Nafion 117 was immersed for 5 minutes in the above casting solution. A cross-linking solution of 5 vol.% glutaraldehyde, 0.12 vol.% HCl, and remainder acetone solution was made. The membrane was immersed in the above solution for 48 hours at 40° C for the purpose of enhancing the mechanical strength of the membrane. It was then washed with high purity water, American Chemical Society (ACS) Reagent grade water, 3 times. Finally, the membrane was sulfonated in a mixture of chlorsulfonic acid and glacial acetic acid of volumetric ratio of 3:10 at 50° C for 6 hours to improve proton conductivity. At the end of the sulfonation treatment, the membrane was washed with high purity water 3 times [12].

The process of creating the Nafion/PVA composite membrane faced numerous difficulties. The first consisted of the membrane curling up into a scroll when placed in the casting solution, which prevented the membrane from being uniformly exposed to the casting solution. Tweezers were used in effort to flatten the membrane so that the entire membrane could be submerged in the solution. This was a pseudo effective method in that after several tries, the membrane was flattened out, but, at the end of the process, scratches were noticed on the membrane. Because Nafion is a delicate material, scratches on the membrane location, where the reaction would be occurring, would not be acceptable. Two different methods were used to prevent the curling of the membrane on initial contact with the casting solution. One method was to use tweezers to unroll the

membrane as described previously, but special efforts were made to grab only the outer edges of the membrane where the scratches would have no effect on the membrane performance. The second method was to use a glass weight, such as a beaker, with a smaller diameter than the container holding the casting solution, and place it on top of the membrane before placing into the casting solution. This would hinder the membrane from curling up too much. In the end, the second method was used, and the first method was used when necessary.

Another problem that was encountered consisted of the membrane drying out during the cross-linking process as seen in Figure 4-8.

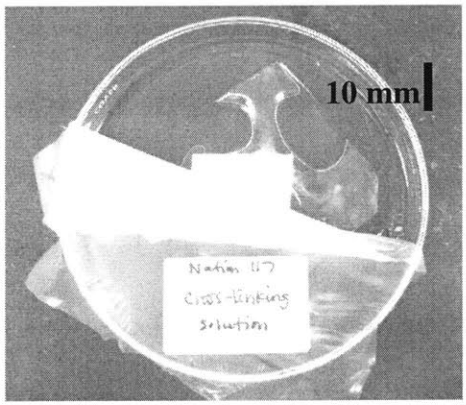

Figure 4-8 Dried out membrane during cross-linking

It was observed that in order to prevent the cross-linking solution from drying out while in the oven for 48 hours, an initial minimum of 50 ml of the cross-linking solution in a beaker with 65-mm diameter was needed. It is suggested that the solution be checked every few hours to make sure that it does not dry out. In addition, rather than an open glass container, putting the solution in a covered glass container prevented the solution from evaporating quickly.

The greatest problem seemed to occur during the sulfonation step. Chlorsulfonic acid is a very strong acid that reacts violently with many substances, including water.

Thus, dunking the membrane into the sulfonation treatment containing chlorosulfonic and glacial acetic acid, following the high purity water washing process, causes the membrane to react violently. In addition, it was learned that only glass could be used to measure or store these acids; in fact, the entire container, including the top, should be made of glass.

The interesting observation is that having repeated the exact same procedure several times, there were various discoloration differences in the final outcome of the membrane as seen in Figure 4-9.

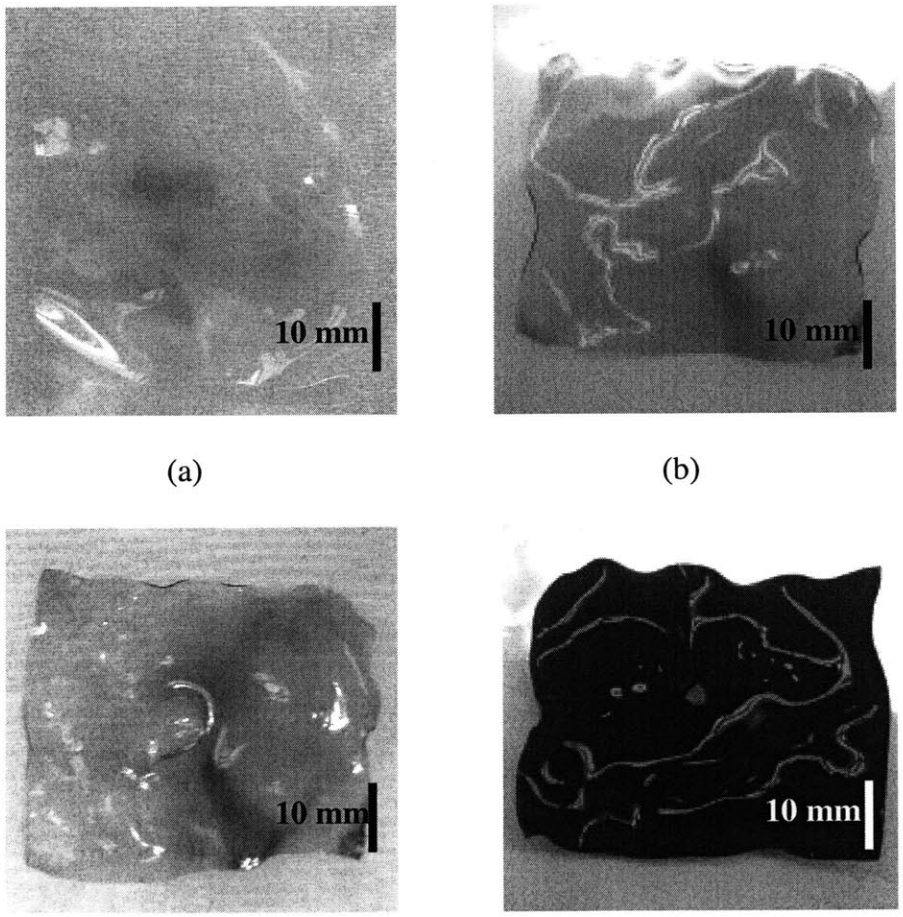

(a) (b)

(c) (d)

Figure 4-9 Various membranes after final sulfonation treatment

It was hypothesized that the difference in the outcome of the membranes could be due to the changes in the Nafion membrane itself overtime. To test this, a new membrane was purchased and experimented on. Although the discoloration was not as drastic as Figure 4-9d, discolorations were still present. It was concluded however, that the effects of discoloration to the performance of the fuel cell are unknown. Thus, the decision was made to continue to use the membrane to create an MEA for testing.

Lastly, there were problems with the planarity of the final dried membrane. As seen in Figure 4-9, the membranes do not have a flat surface. Thus a similar tactic used to flatten the membrane when dipping into the cross-linking solution was used: to dry, the membrane was sandwiched in between to pieces of glass. Thus a flat membrane was produced as seen in Figure 4-10.

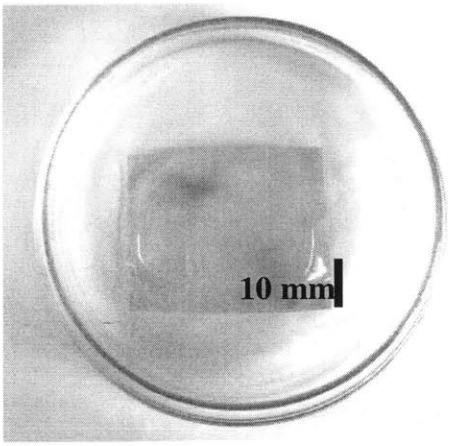

Figure 4-10 Final PVA/Nafion membrane

However, hot-pressing changed the color and planarity of the membrane as seen in Figure 4-11. The discolorations became darker and the applied heat slightly warped the membrane, but it did not affect the process of putting the MEA into the fuel cell for testing.

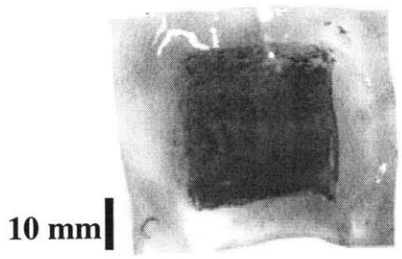

Figure 4-11 MEA made of PVA/Nafion membrane

4.2 Passive Cathode Fuel Cell

A fuel cell with active area of $5cm^2$ with a serpentine flow as seen in Figure 4-12 was purchased from Electrochem Inc.

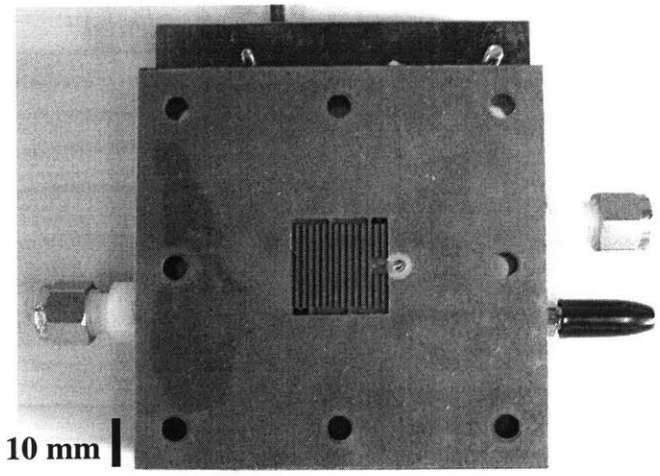

Figure 4-12 Electrochem Inc. open fuel cell with serpentine flow

A passive cathode fuel cell was constructed in order to decrease the overall volume of the fuel cell as seen in Figure 4-13.

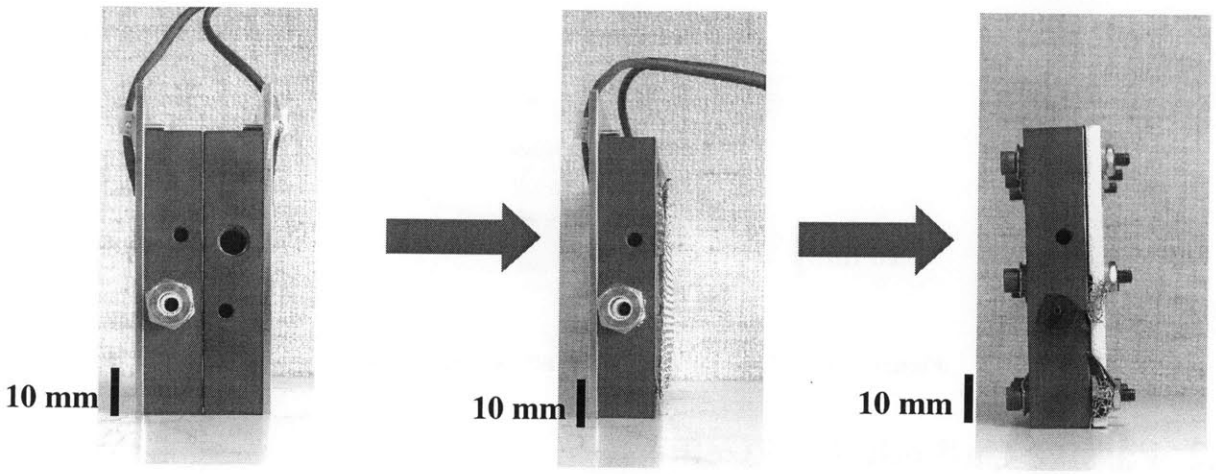

Figure 4-13 Volume decrease in passive fuel cell

The graphite block of the cathode side was replaced with a wire mesh and in the final design, the addition of an aluminum plate as discussed in Section 3.3.2. The final construction of the passive fuel cell can be seen in Figure 4-14.

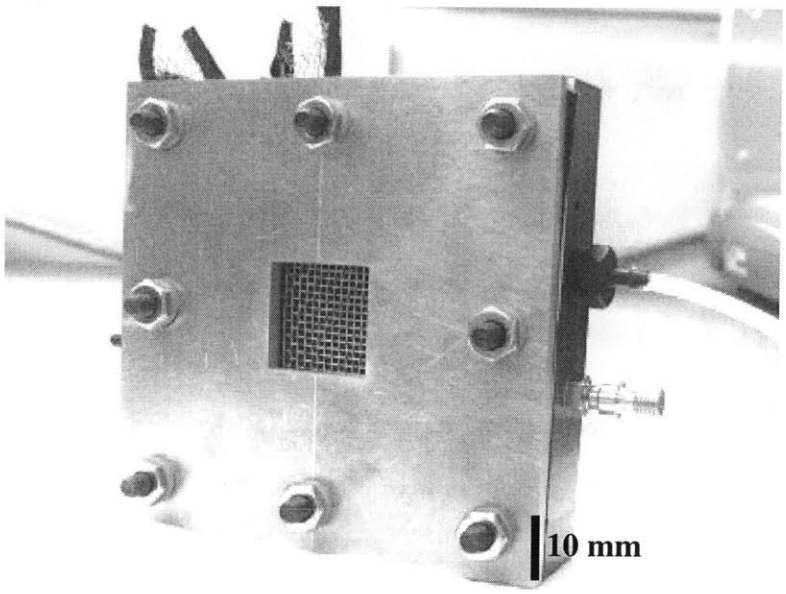

Figure 4-14 Passive fuel cell, final construction

4.3 Test setup

4.3.1 Initial Test setup

The performance of the fuel cell was originally tested by a simple setup as shown in a schematic diagram, Figure 4-15.

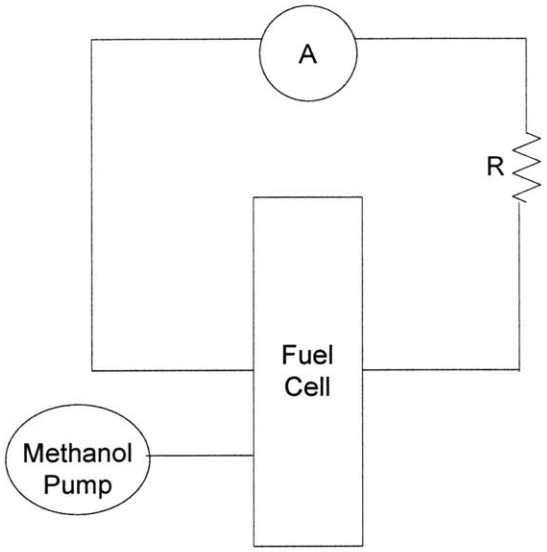

Figure 4-15 Schematic of initial test setup

The resistor, R, in Figure 4-15 was interchanged with various resistors from 1 to 325 ohms at intervals of approximately 25-50 ohms. The current, I, was measured from a Fluke 79 multimeter, which was connected in series with the circuit above, and the voltage was measured across the fuel cell.

The voltage drop, ΔV, is modeled as:

$$\Delta V = R \cdot I \qquad \textbf{4-1}$$

A diaphragm micro pump was used as seen in Figure 4-16.

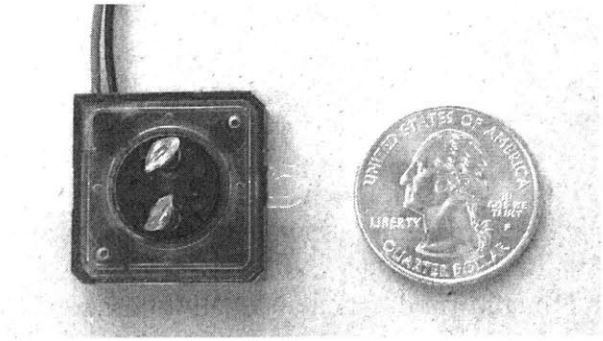

Figure 4-16 Methanol pump

A pump controller as seen in Figure 4-17 was used to vary the flow rate by adjusting the frequency and voltage.

Figure 4-17 Pump controller

The basic test setup in its entirety can be seen in Figure 4-18.

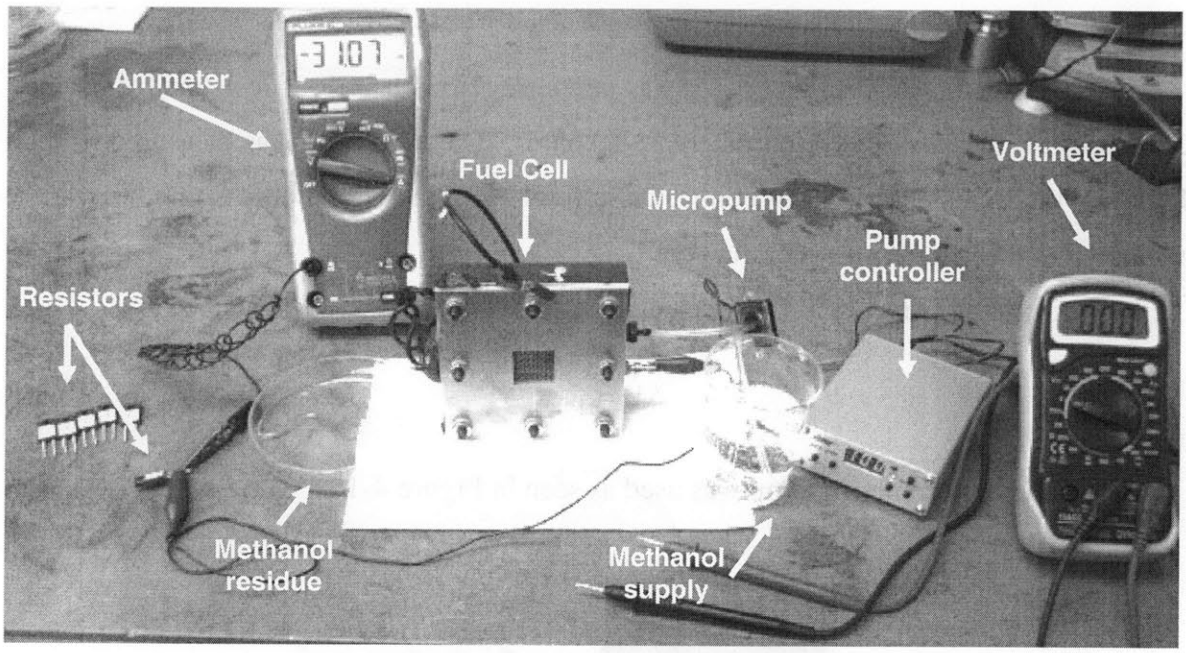

Figure 4-18 Basic test setup

After a preliminary experimental run on the test setup, a potentiostat, Solartron SI 1287, was used in efforts to confirm the data obtained for the setup in Figure 4-18. It was discovered, however, that the voltage and current readings did not match. This was due to the internal resistance of 11mV/mA or 0.03 mV/mA of the mulitemter, depending on the mA or A setting, respectively. The schematic of the test setup from Figure 4-18 was

changed to that of Figure 4-19 with the addition of a resistor, $R_{Ammeter}$, which represents the additional resistance that the ammeter contributes to the circuit.

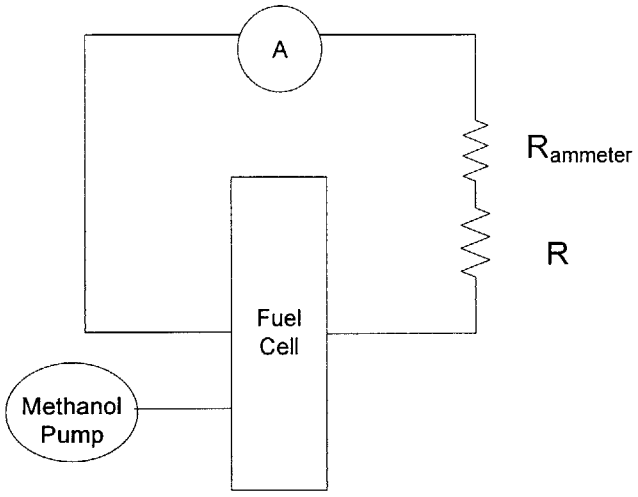

Figure 4-19 Revised Schematic of initial test setup

The voltage drop across the fuel cell from Equation 4-1 was thus re-modeled as:

$$\Delta V = (R_{Ammeter} + R) \cdot I \qquad \textbf{4-2}$$

The actual voltage had to be adjusted by subtracting the voltage from $R_{Ammeter}\, I$. In the end it was decided that using a potentiostat would be more accurate.

4.3.2 Potentiostat test setup

A potentiostat, Solartron SI 1287, as seen in Figure 4-20, and the accompanying Coreware software was used to change the potential of the fuel cell while each corresponding current was recorded.

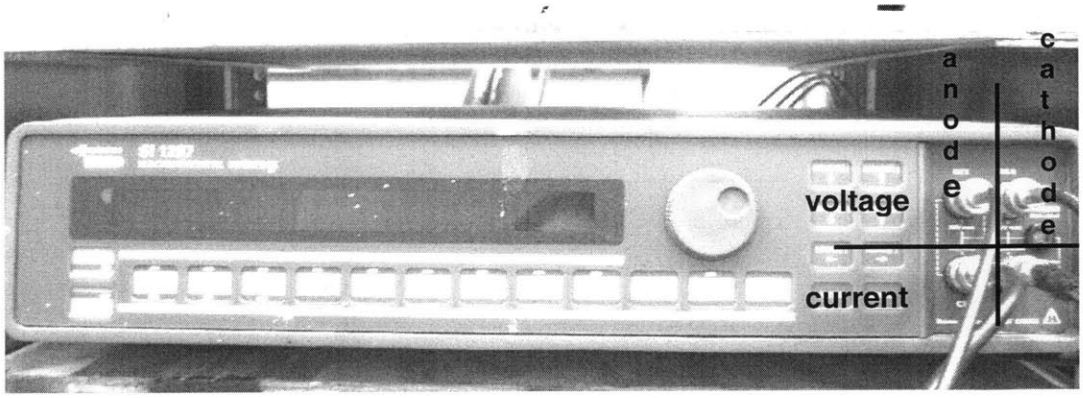

Figure 4-20 Solartron SI 1287 and connection

The voltage and current connectors at each electrode were combined and connected from the potentiostat to the corresponding fuel cell electrode as a single connection. Figure 4-21 shows the entire setup with the single voltage and current connection from the potentiostat for both the anode and cathode.

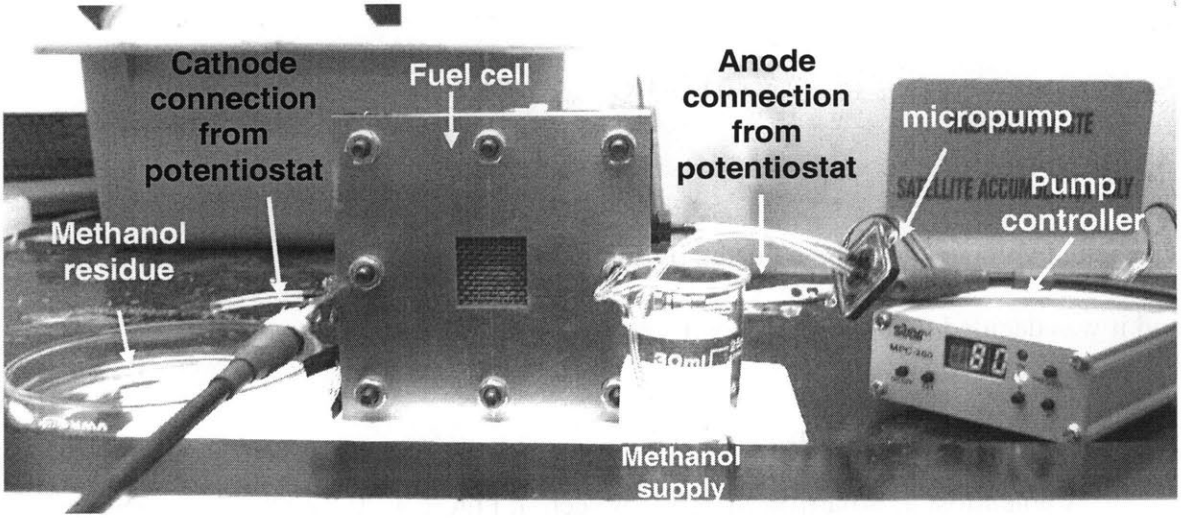

Figure 4-21 Potentiostat test setup

4.3.3 Additional test setup

Of the parameters that were changed in testing the fuel cell, one in particular required changes in the test setup. The extra setup is the addition of pure oxygen to the cathode side of the fuel cell. An emergency oxygen tank that delivers pure oxygen was

used to supply the oxygen to the cathode side. The face mask was attached to the fuel cell as shown in Figure 4-22 with rubber straps and reinforced with parafilm and tape.

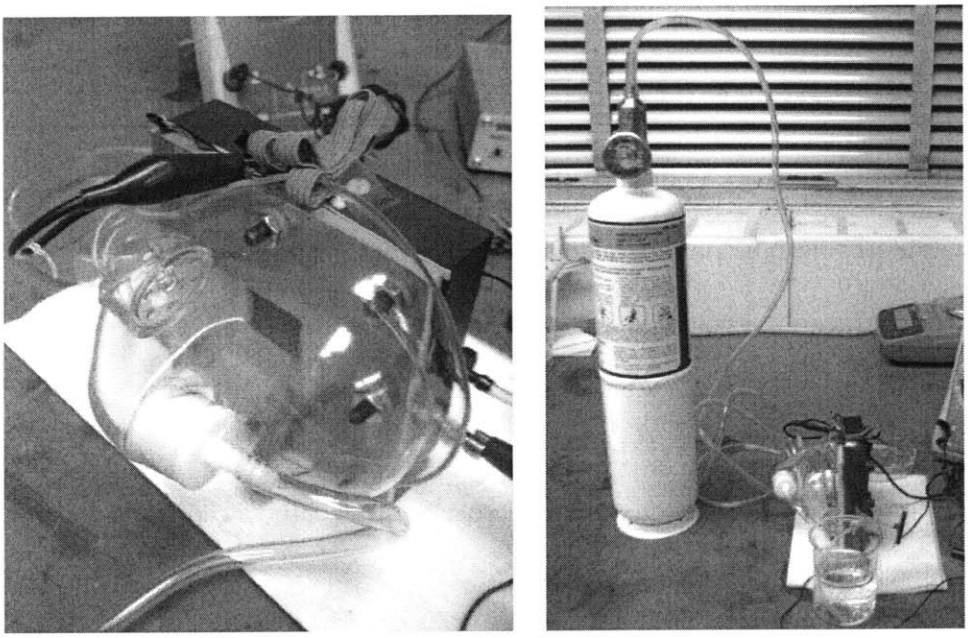

Figure 4-22 Oxygen setup

Chapter

5 Results and discussion

All results have been obtained form an average of three trials each. 3M methanol was used as a standard methanol concentration for reasons discussed in Section 3.3.3. The experiments were all performed at the room temperature of 22 °C.

5.1 Prefabricated MEA results

Using the potentiostat, the voltage across the fuel cell was adjusted from 0.1 to 0.5 V with increasing increments of 0.1 V, while the corresponding current for each voltage was recorded.

5.1.1 ElectroChem Inc. vs. Fuel cell store MEA

Two pre-fabricated MEAs were purchased from two different manufacturers: Electrochem Inc. and the Fuel Cell Store. Both MEAs had an active area of $5cm^2$ and an electrolyte membrane of Nafion 117 and catalysts loadings of $4mg/cm^2$ for both the anode and cathode. However, they had different catalysts and backing layers as summarized in Table 5-1. In addition, the GDLs from the Fuel Cell Store were separated from the MEA and to be inserted during fuel cell assembly, whereas the GDLs from Electrochem Inc. were made hot-pressed onto the MEA.

Table 5-1 MEA characteristics of ElectroChem Inc. and Fuel Cell Store MEA

	Cathode		Anode	
	catalyst	backing	catalyst	backing
Electrochem	4mg/cm^2 Pt (40 wt% Pt/C)	carbon cloth	4mg/cm^2 Pt/Ru (40 wt% Pt, 20 wt% Ru/C)	carbon paper
Fuel Cell Store	4mg/cm^2 Pt black	Etek ELAT	4mg/cm^2 Pt Black/Ru	carbon cloth

Overall, the MEA from the Fuel Cell Store had higher performance than the MEA from ElectroChem Inc. Figure 5-1 shows an example of this trend for experiments run with 3M methanol at a flow rate of 1.5ml/min. For a given current density, the power density is greater by a factor of two or more.

This difference in performance could be due to several factors. The different backing layers could contribute to the method and speed with which reactants and products are passed in and out of the fuel cell affecting the speed of the electrochemical reaction. A greater contributor to the difference in performance could be the use of different catalyst material, especially the anode side. In DMFCs, one of the greatest detriments to efficient performance is the slow reaction speed at the anode. The catalyst used by the Fuel Cell Store has been reported up to date as the most efficient anode catalyst for DMFCS [4]. Despite their relative differences in performance, both MEA performances were similar to that of the reported results of others, such as Shimizu *et al.*, who tested passive cathode fuel cells [20].

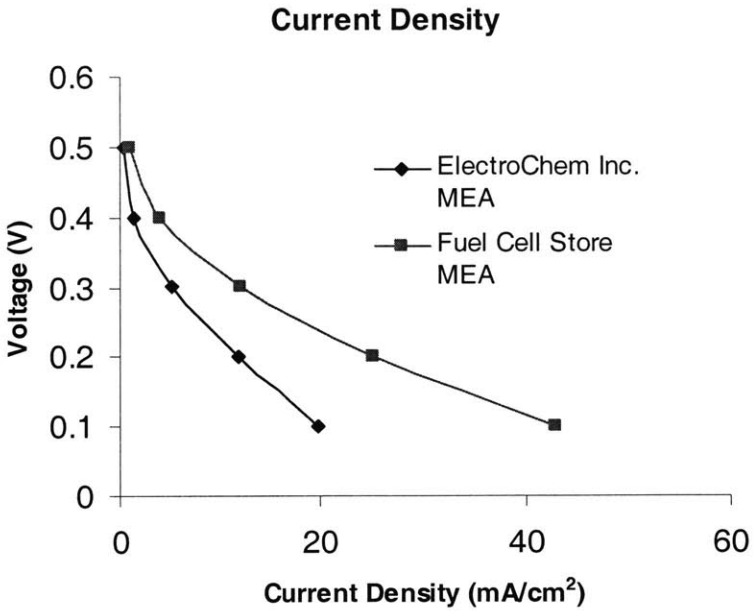

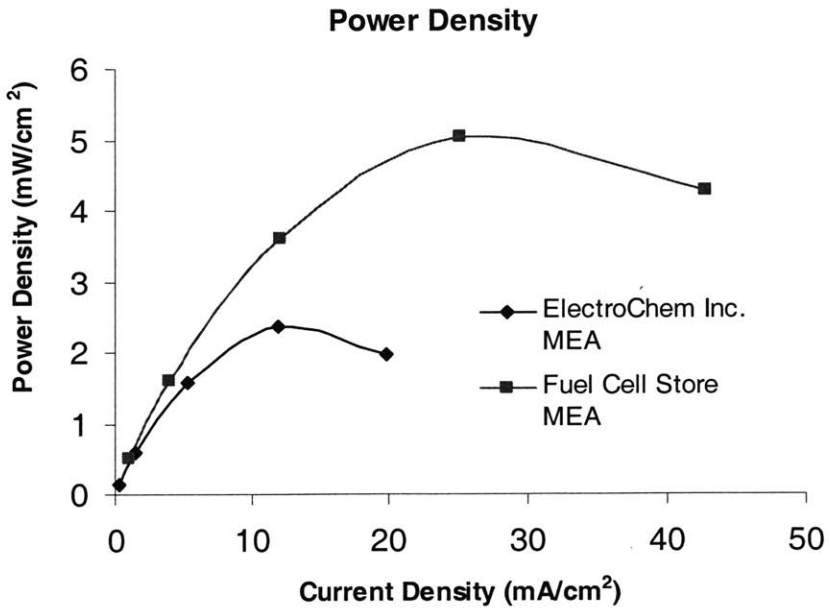

Figure 5-1 Performance curves: ElectroChem Inc. vs. Fuel Cell Store

Further performance curves with varying methanol flow rate, oxygen and methanol concentration, and GDL of the Fuel Cell Store MEA will be presented and discussed in the following sections.

5.1.2 Methanol flow rate

The methanol flow rate to the fuel cell was varied to test the effect on the performance; 0.5 ml/min, 1.5 ml/min, and 3 ml/min were tested. Although the pump capacity allowed up to a 6 ml/min flow rate, leakage of methanol was observed for flow rates beyond 3ml/min.

With increased flow rate, there is increased pressure. Increased pressure is expected to force more reactants at the reaction sites and thus the increase in the reaction speed and increase in performance [18]. However, the results in Figure 5-2 show that increasing the methanol flow rate at the anode does not significantly change the performance of the fuel cell.

The minimal variation between the flow rates could be attributed to methanol crossover. Although higher performance is expected at higher flow rates, fuel crossover is also more likely in this region. The benefit of a higher flow rate could be negated by fuel crossover effects, possibly providing an explanation for the negligible difference in performance between the varied methanol flow rates. Based on these results, it was decided to operate the fuel cell at 1.5 ml/min methanol flow rate for the remainder of the experiments because its power density is slightly greater than the 0.5 ml/min flow rate, but it would conserve more fuel than the 3 ml/min flow rate.

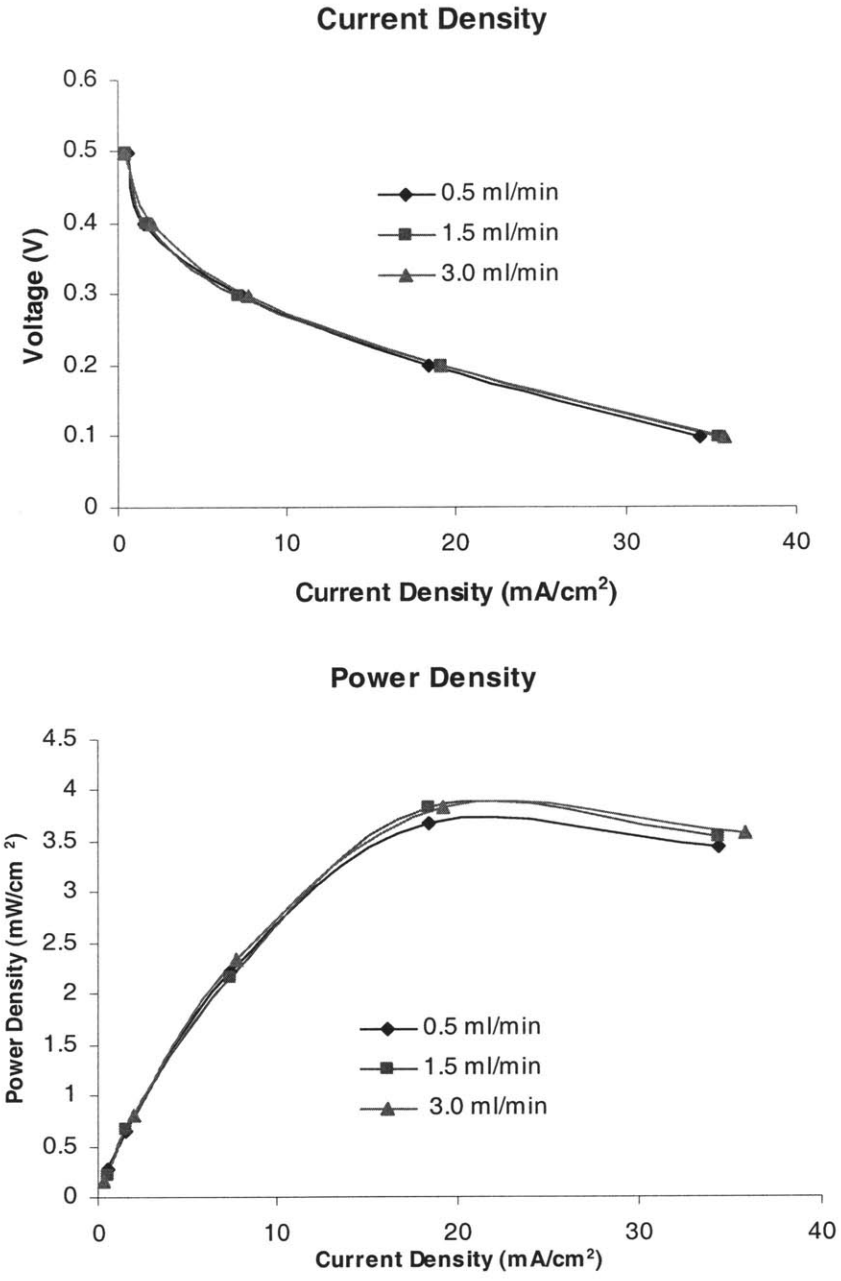

Figure 5-2 Performance curves: effect of methanol flow rate variation

5.1.3 Oxygen concentration

Another parameter that was altered for increased performance was increasing the concentration of the cathode reactant, oxygen. Le Châtelier's principle can be used to predict that the increase of reactant concentration, in this case oxygen, would increase the

products and thus, increase the performance of the fuel cell [22]. To best simulate a passive fuel cell in a mobile application, the ambient air, which contains 20% oxygen, was used when running tests on the fuel cell. However, in order to understand and narrow down the factors that contribute to the inefficiencies of the fuel cell, pure 100% oxygen was used at the cathode as the reactant. This was done by using an emergency oxygen tank and placing the mask over the fuel cell cathode as discussed previously in Section 4.3.3. The pure oxygen was delivered to the fuel cell at 6 liters per minute. The results in Figure 5-3 show that increased oxygen concentration increases the performance of the fuel cell by approximately a factor of 1.5.

With greater oxygen concentration, the increase in performance is expected because the reactants can be consumed quicker in a concentrated amount, similar to that which was expected with increased reactant flow rate. However, when considering a mobile device, having access to pure oxygen will increase the volume of the fuel cell, which is not favorable. Thus it would be ideal if alternative methods were considered to increase the performance without increasing the volume of the fuel cell or a method to increase the oxygen concentration without requiring pure oxygen was considered. One possible way to do this would be by increasing the partial pressure of oxygen in air.

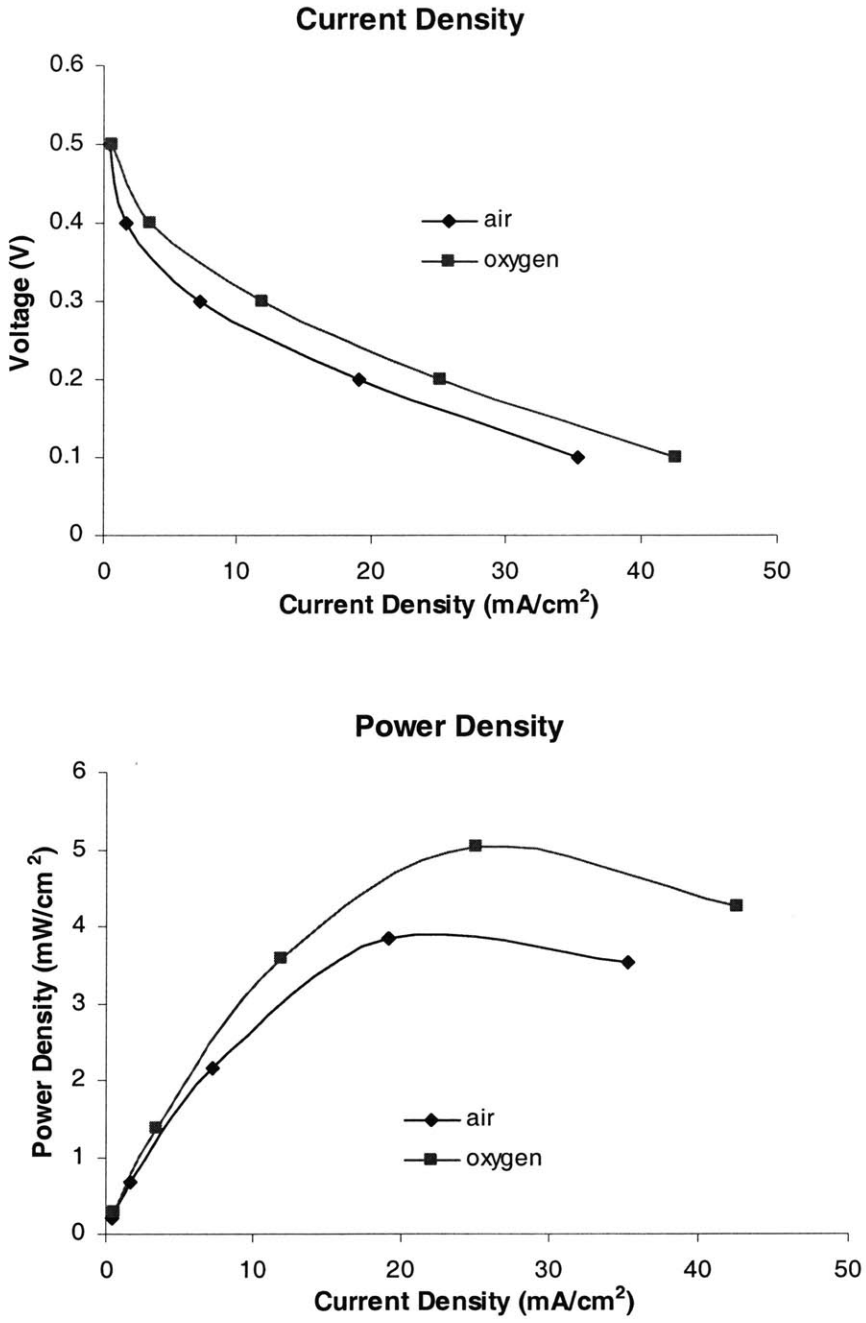

Figure 5-3 Performance curves: effect of oxygen concentration

5.1.4 Methanol concentration

Increasing methanol concentration is a positive change that could be made without significantly increasing the volume of the fuel cell. However, as discussed in

Section 2.3.2, methanol crossover is a major factor in decreased efficiency in a DMFC. Thus, merely using 100% methanol will not solve this problem. In fact, using 100% methanol damaged the MEA when running experiments. In one case, it even burned off a part of the MEA as seen in Figure 5-4.

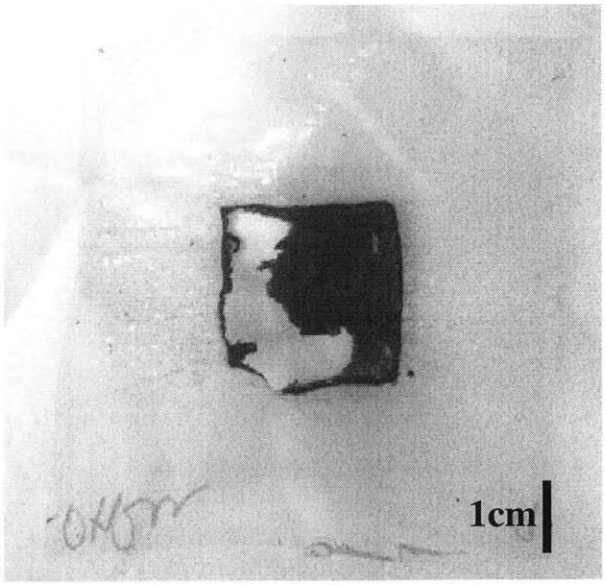

Figure 5-4 Damaged MEA due to 100% methanol

The damaging effect of the methanol on the MEA was visibly identified when the methanol exit flow would be a creamy milk color rather than the clear transparent liquid that methanol is supposed to be. 100% methanol concentration was tried three times, but each time caused failure in the membrane. Thus, 1M, 3M, and 15M, which is equivalent to approximately 50% methanol, were used to observe the effects on the performance as seen in Figure 5-5 testing an MEA from the Fuel Cell Store.

The performance curves show that using 1M methanol results in higher power density than 3M or 15M methanol by approximately a factor of 2. Although not as much of a margin, using 15M methanol for the fuel cell produced the lowest performance. These results suggest that methanol crossover is a likely cause of the decreased

performance in the fuel cell. Thus the need and importance of preventing methanol crossover in order to increase performance has been confirmed by the results of this experiment.

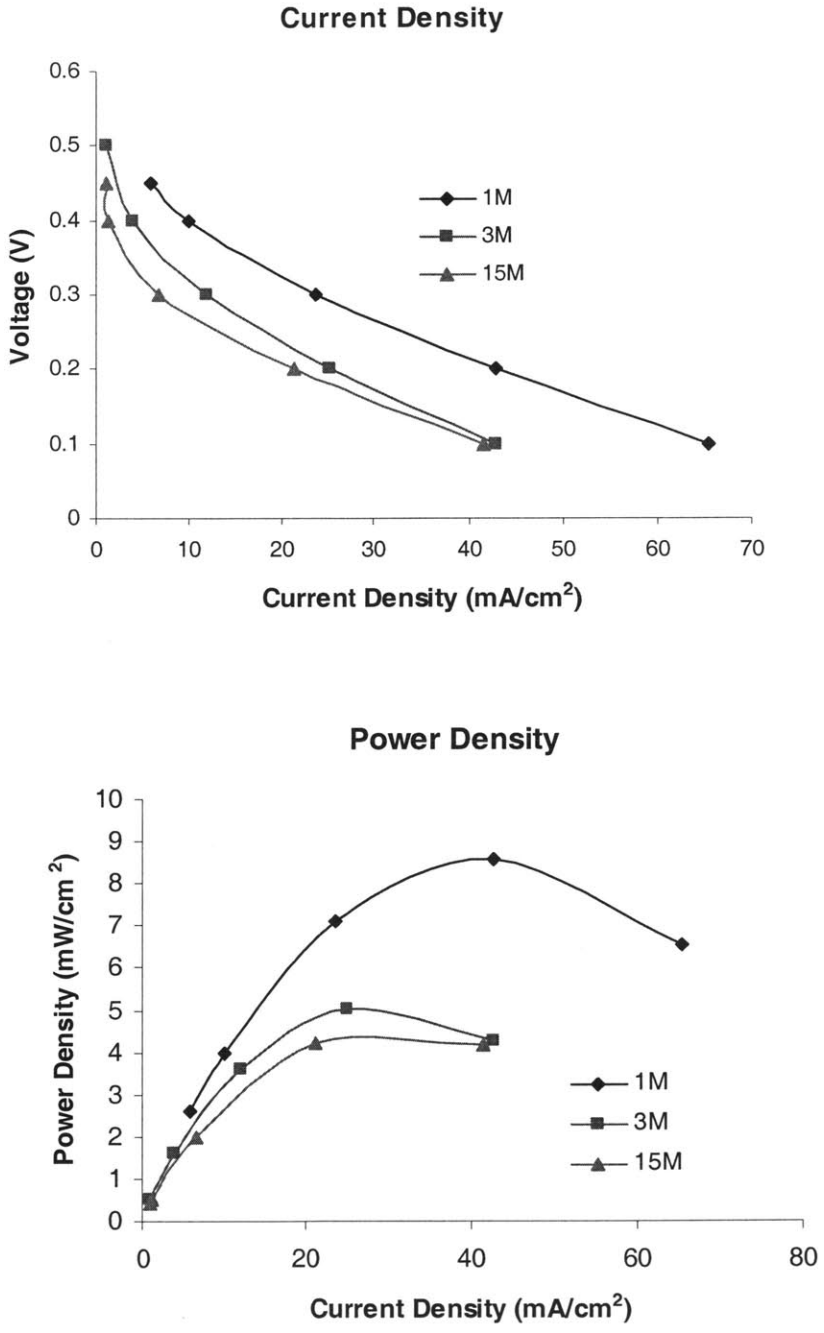

Figure 5-5 Performance curves: effect of variable methanol concentration

5.1.5 Microporous Layer

As discussed in Section 3.2.1, an MPL was decided to be used to prevent flooding at the cathode and thus increase the performance of the fuel cell. An MEA from the Fuel Cell Store was tested by varying the cathode GDL: ELAT from E-Tek, carbon paper with an MPL from SGL, and carbon cloth. The performance results are seen in Figure 5-6 for the MEAs operated using 3M methanol fed at 1.5ml/min. Despite the findings from Section 5.1.4 that showed 1M methanol to have higher performance than 3M, the methanol concentration was kept at 3M in order to keep as many experimental parameters as constant as possible throughout all of the tests.

It was expected that the ELAT cloth and SGL carbon paper would be most effective in preventing flooding, and thus show an increase in performance compared to the regular carbon cloth GDL. However, as seen in Figure 5-6, this is not necessarily the case. The SGL carbon paper and regular carbon cloth as the cathode GDL had better performance than the ELAT cloth. Unfortunately, because the ELAT cloth and SGL carbon paper are both proprietary materials, their compositions cannot be analyzed. However, it can be deduced from the results above that for a fuel cell operating at the given conditions, the optimum hydrophobicity was better achieved by the SGL carbon paper and plain carbon cloth than the ELAT cloth. Given that the SGL carbon paper is more expensive than plain carbon cloth and they have very similar performance results, it was concluded that using plain carbon cloth as a GDL was preferable.

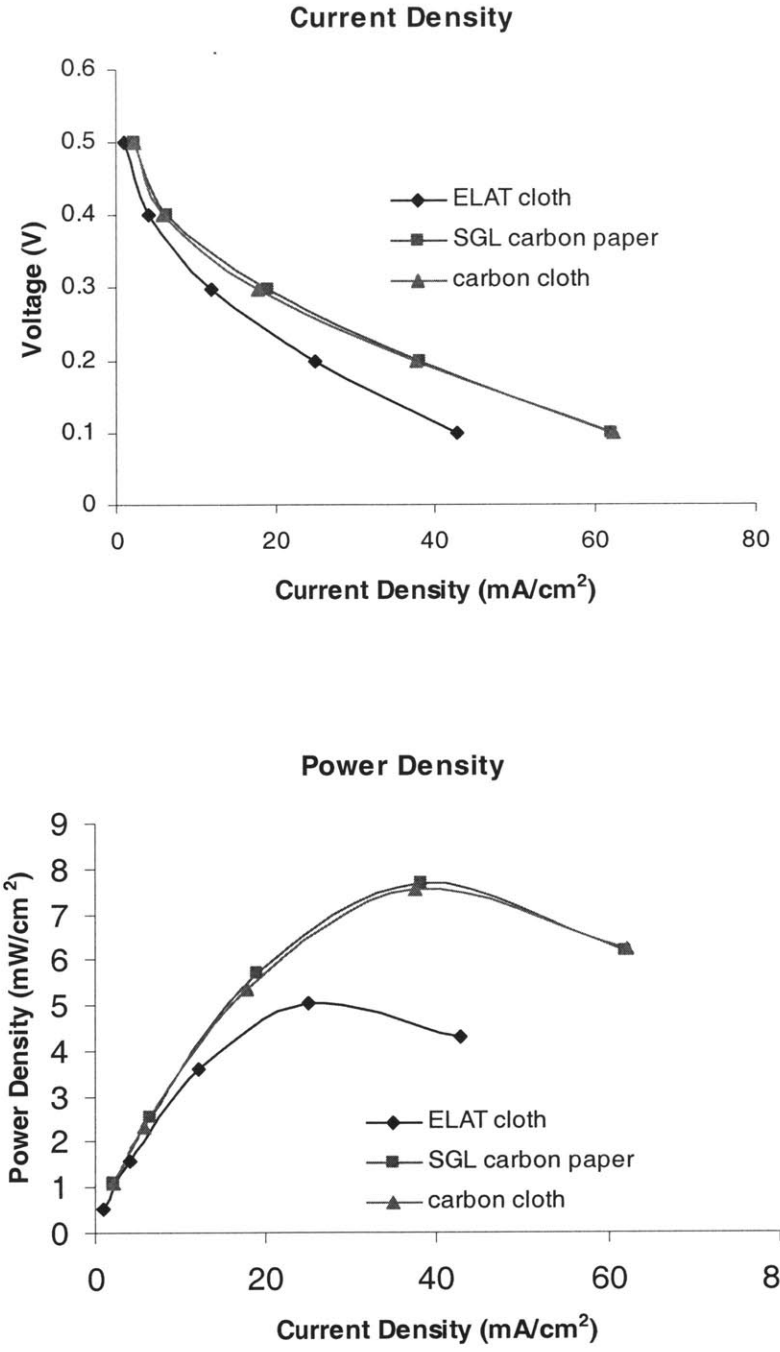

Figure 5-6 Performance curves: Effect of variable cathode GDL

This conclusion raised a question, however, on whether or not flooding was even a problem in the fuel cell that was being tested. Flooding was not visible to the naked eye at any time except when the flow rate of the methanol was increased to 6ml/min, the

maximum flow rate possible by the pump. However, this was flooding of the methanol and not due to the excessive water produced. Thus, based on the results, it has been concluded that at the current methanol concentration and flow rate, flooding is not a major problem and plain cloth can be used as a GDL.

5.2 Experimentally fabricated MEA results

Two types of MEAs with different membranes were fabricated: MEAs with standard Nafion 117 and MEAs with a modified PVA/Nafion membrane. The two purposes of these MEAs were to analyze the results of the experimentally fabricated standard MEA and to compare it to the modified MEA. The Pt catalyst loading for the cathode was between 0.75 and 1 mg/cm^2 and the Pt catalyst loading for the anode was between 2 and 2.3 mg/cm^2. 3M methanol at 1.5 ml/min flow rate was used for the following experiments.

5.2.1 Standard Nafion 117 MEA

Three MEAs were fabricated with Nafion 117 following the procedure in Section 4.1.1. The results shown in Figure 5-7 showed slight variations in performance between the MEAs, but the overall patterns observed in the performance curves were expected.

The most important thing to note, however, is the smaller current density and power density output of the fuel cell of the experimentally fabricated MEAs. In comparison to the prefabricated MEAs, the current and power densities are lower by approximately 2 orders of magnitude. However, the current density curves show that the voltage range is only lower by a factor of ½. This shows that fuel crossover is a major factor on the performance. When fuel crosses over, the electron conduction is occurring through the electrolyte, when the electrolyte is only supposed to be conducting ions.

Thus, there is a decrease in current, sometimes a very significant decrease in current, similar to what happens when a circuit is shorted.

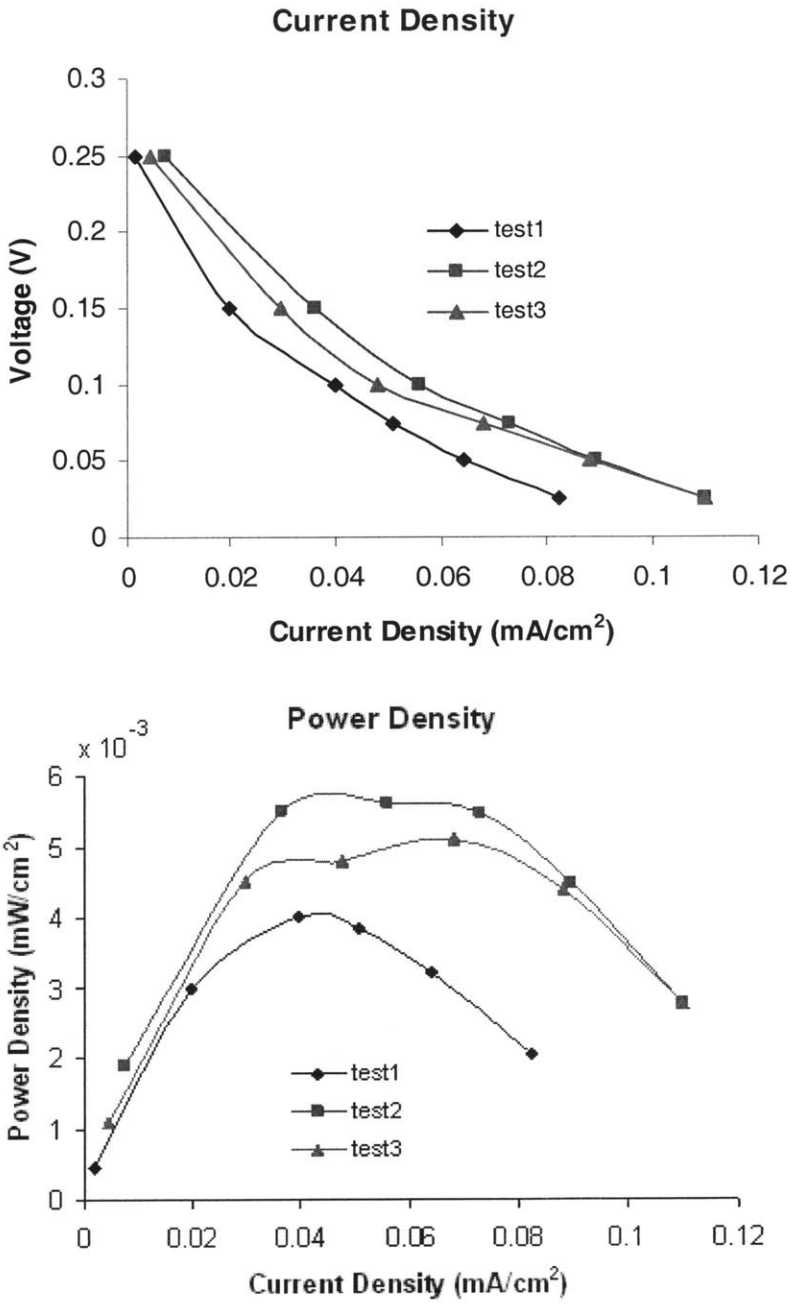

Figure 5-7 Performance cuves: fabricated MEA with Nafion 117

At first glance, the fuel crossover could be attributed to the poor membrane. However, since Nafion 117 was used without alterations, this seemed unlikely. The

greatest room for variability between the experimentally fabricated MEA and prefabricated MEA is the catalyst fabrication and application process.

If the catalyst inks are either fabricated or applied incorrectly, this could affect the fuel cross over effect. This is because if the catalysts are not functioning properly, the reaction at the electrodes are slowed down. When the reaction at the anode is slowed down, this would also slow down the methanol from being consumed, thus forcing the methanol through the membrane without reacting. The results in the following section further strengthen this argument.

5.2.2 Modified PVA/Nafion MEA

Three MEAs were created with the PVA/Nafion membrane following the procedures from Section 4.1.4. The results in Figure 5-8 compare the modified MEAs to standard MEAs made of Nafion 117. This was done by taking the average performance of the three experimentally fabricated MEAs for each the modified and standard types.

The current density plot shows that the modified PVA/Nafion membrane outputs very low voltage but higher current than the regular MEAs made of Nafion 117. Thus, it confirms that the PVA/Nafion modified membrane has positive effects on preventing methanol crossover and increasing performance of the fuel cell. However, the low voltage shows that other losses are taking place due to the modified PVA/Nafion membrane. A possible explanation for this is the negative effect the PVA/Nafion modification has on proton conductivity. A final sulfonation step was used to increase proton conductivity of the modified membrane, but this step is what also caused the discoloration in the membrane and is what could be the reason for the low voltage range. Other methods of increasing proton conductivity could be used on the PVA/Nafion

membrane to test whether or not it is the actual cause for the low voltage. Or an entirely different method for decreasing methanol crossover could be tested for possible higher overall performance.

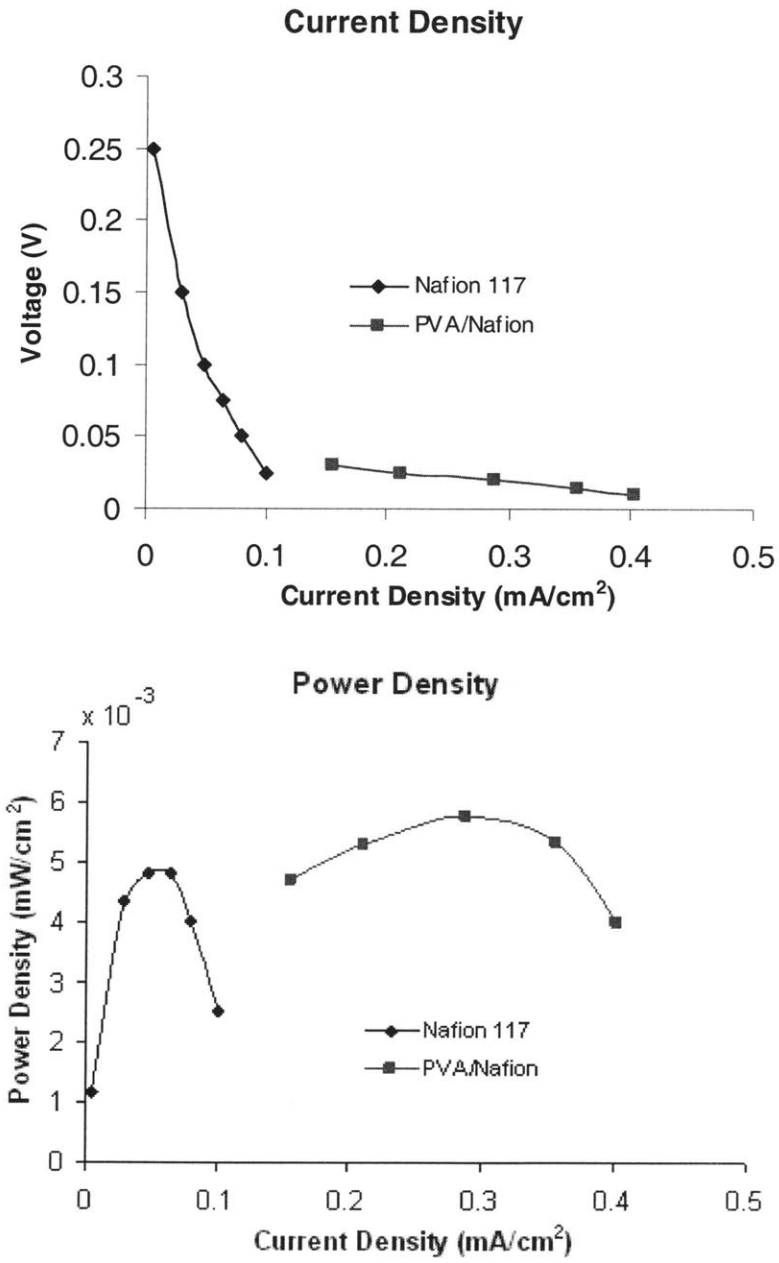

Figure 5-8 Performance curves: Nafion 117 vs. PVA/ Nafion

5.3 Repeatability

All plots in this chapter demonstrated repeatability. All plots were derived from an average of three points that did not vary by more than 1%. Figure 5-9 shows a sample set of plots from a purchased MEA from Electrochem Inc. that exemplify the repeatability seen in all of the experiments above including the MEAs that were fabricated.

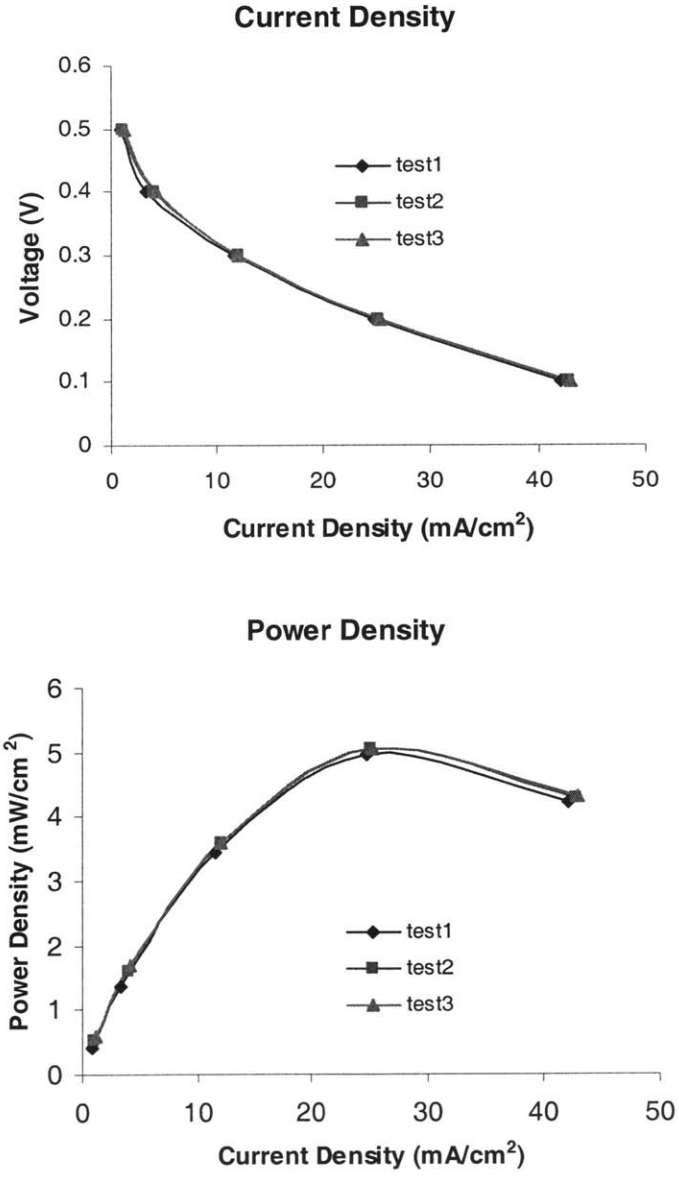

Figure 5-9 Performance curves demonstrating repeatability

CHAPTER

6 Circuit design of fuel cell - capacitor hybrid

6.1 Hybrid technology

The advantage in a fuel cell hybrid system is that the fuel cell works quite close to its maximum power at all times. When the total system power requirements are low, the extra electrical energy is stored in a rechargeable batter or capacitor. When the power requirement is higher than what the fuel cell can provide, then the energy is taken from the battery or capacitor [4].

A very widely used hybrid technology is the hybrid vehicle. When the car is first started, or at the initial reaction, the battery provides power to the electric motor which provides the initial burst of energy as shown in Figure 6-1.

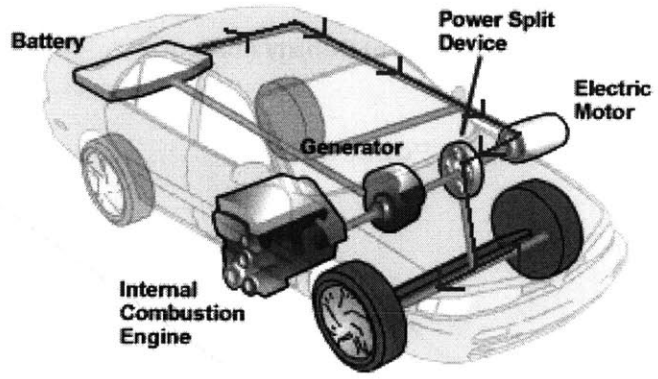

Figure 6-1 Startup of Hybrid Car [23]

This will continue even at low speed cruising until the battery capacity starts to decrease to a certain level. Then the internal combustion engine kicks in, recharging the battery and providing power for the car as shown in Figure 6-2.

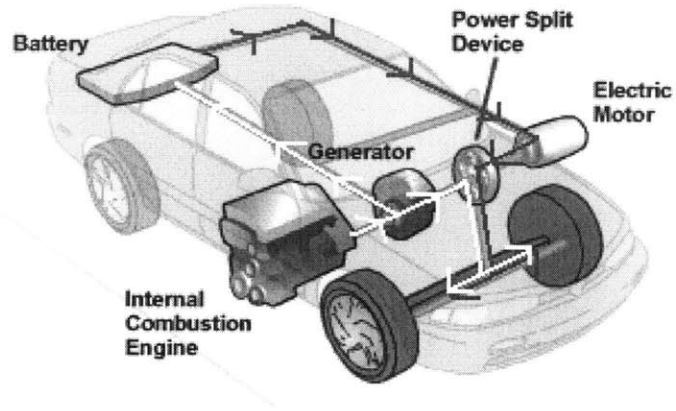

Figure 6-2 Low Speed Cruising of Hybrid Car [23]

In high speed cruising it is the opposite. The engine provides all of the power as shown in Figure 6-3.

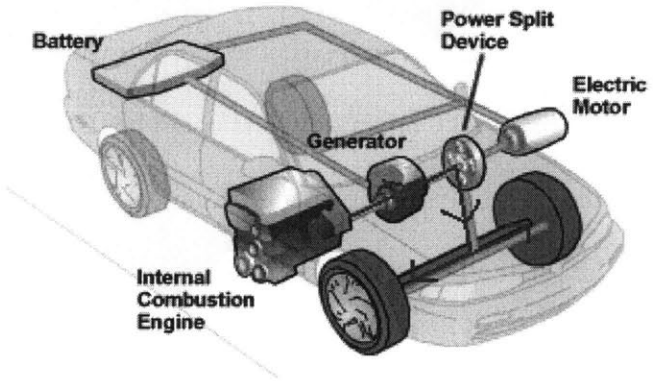

Figure 6-3 High Speed Cruising of Hybrid Car [23]

And at high acceleration, or after a long time, the electric motor powered by the battery will kick in to provide any additional bursts of power that is needed as shown in Figure 6-4.

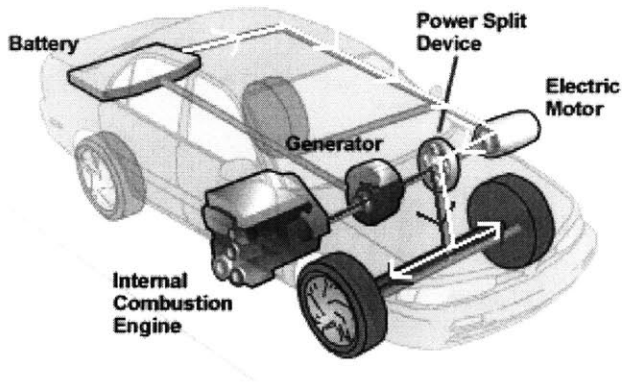

Figure 6-4 High Acceleration of Hybrid Car [23]

This is very similar to the hybrid use in a cellular phone as shown in Figure 6-5. At the initial startup and while the cellular phone is on but not in use, only the battery would be powering the device. If it has been idle for awhile, after a long time, the battery capacity might start to be very low, in which case the fuel cell would kick in and provide power while recharging the battery. Conversely, one could be talking on the phone, in this case the fuel cell would be the main power source, and after awhile if this application needs more power than the fuel cell can provide, the battery will kick in.

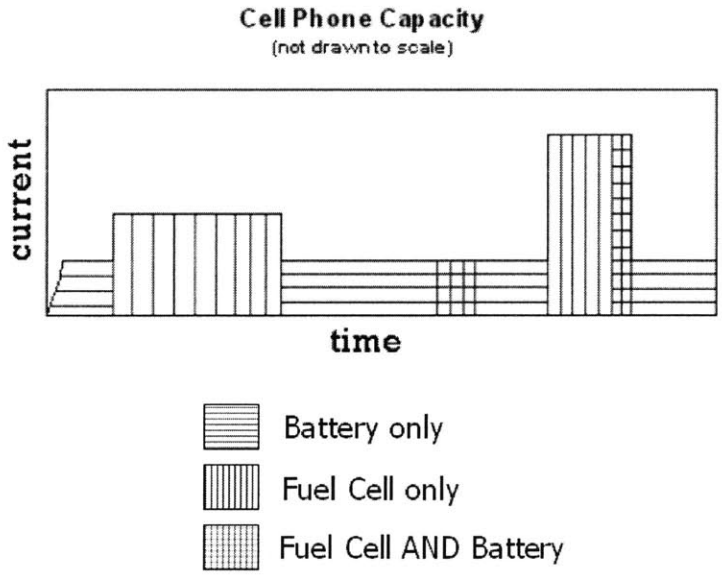

Figure 6-5 Hybrid Use in Cellular Phones

6.2 System requirements

A DMFC – Capacitor hybrid demo was designed in collaboration with Victor Sinow. Ideally, an actual fuel cell would power this demo, but because there was only one fuel cell, whereas in an actual application you would have a stack of several fuel cells, it did not provide sufficient voltage for this demo. Instead a power supply, providing 2.5 volts was used to mimic a five cell stack of 0.5 volts per cell.

6.2.1 Power dissipation

In order to create a working demo, a single LED bulb was used to visibly indicate when the power was on. A single green LED that draws approximately 100mW of power was used. In addition, a prototype pump and pump driver that draws a total of 250mW of power was part of the system. With these circuit elements, approximately 350mW of total power was dissipated in this demo.

6.2.2 Voltage regulator design

A voltage regulator for both the voltage from the fuel cell to the pump driver and the fuel cell to the LED was needed. This was because the pump driver operates at 5 V and the LED needs at least 3.5 V, but the fuel cell was approximated to produce only 2.5V. Thus, a step-up converter was used to regulate the voltage to 5V for both cases. A step-up converter or boost converter from Linear Technology, model LTC-3535, was used to build the needed regulator as shown in Figure 6-6.

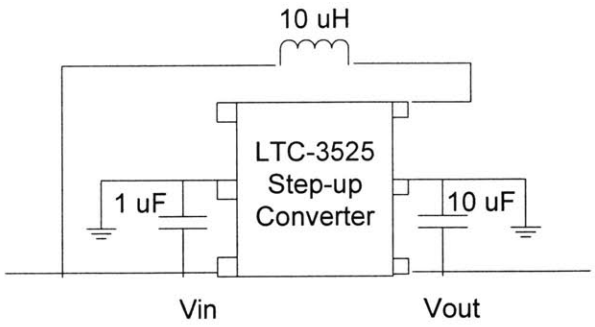

Figure 6-6 Voltage regulator design

Upon suggestion of the manufacturers, an inductor of 10 μH and capacitors of 1 μF and 10 μF were used to connect the boost converter to the rest of the circuitry to create a regulator that will output a steady voltage of 5 V [24].

6.2.3 Capacitance requirement

The demo was created to show the LED bulb light up fully for 1 second. Since the total power dissipated is 100mW, lighting the LED for 1 second would require 100mJ of energy. The LED bulb operates at 3.5 volts so with the voltage regulated to that value, since

$$E = \frac{1}{2} CV^2, \qquad \textbf{6-1}$$

the capacitance can be calculated as 0.016 Farads or 16 mF.

Similarly, for the pump driver which dissipates 240mW, if the shock it needs to start the system is assumed to be 1 second, the required energy would be 240mJ. In actuality, the time it takes for the pump to start the fuel cell would take much longer depending on the flow rate, but due to the limitations of a capacitor, a smaller time frame

was chosen for this demo; if a battery was used, this would not be a problem. From Equation 6-1, the required capacitance can be calculated as .0192 F or 19.2 mF.

A 22 mF or 22,000 μF capacitor from Cornell Dubilier was used for both capacitors. This capacitor provided sufficient capacitance for this demo. However, the large size of the capacitor is not ideal. A supercapacitor from AVX, shown in Figure 6-7, was found as a substitute. The supercapacitor BZ015A503ZA provides more than twice the amount of capacitance, 55mF, and is much smaller.

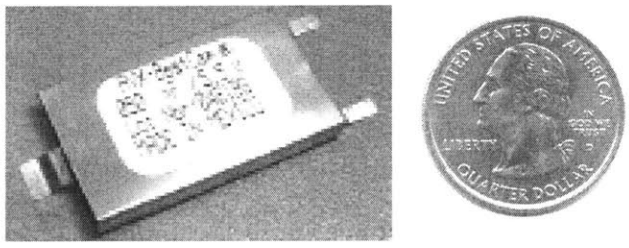

Figure 6-7 AVX supercapacitor BZ015A503ZA

The difference in size of the capacitor and supercapacitor is shown in Figure 6-8.

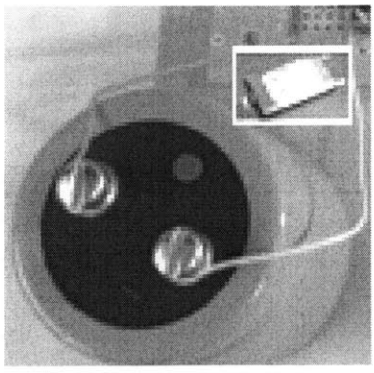

Figure 6-8 Cornell Dubilier capacitor vs. AVX supercapacitor

6.2.4 Hybrid Demo

A full schematic of the fuel cell – capacitor demo, including the regulator circuitry, is shown in Figure 6-9.

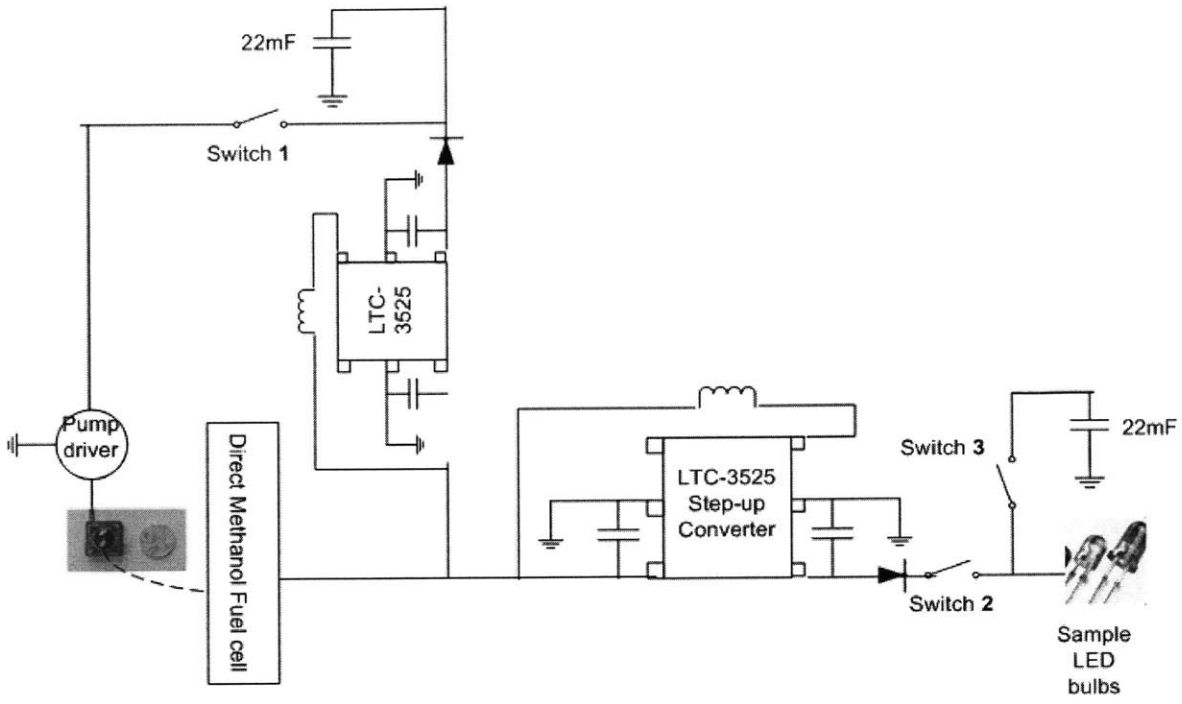

Figure 6-9 Schematic diagram of hybrid demo

The actual fuel cell – capacitor demo setup was built by Victor Sinow and is shown in Figure 6-10.

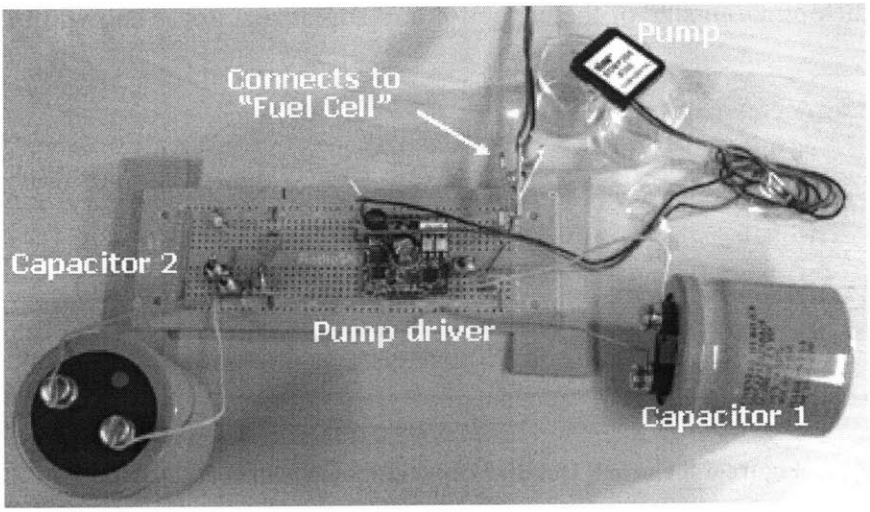

Figure 6-10 Hybrid demo setup

A close up of the pump driver and switches is shown in Figure 6-11.

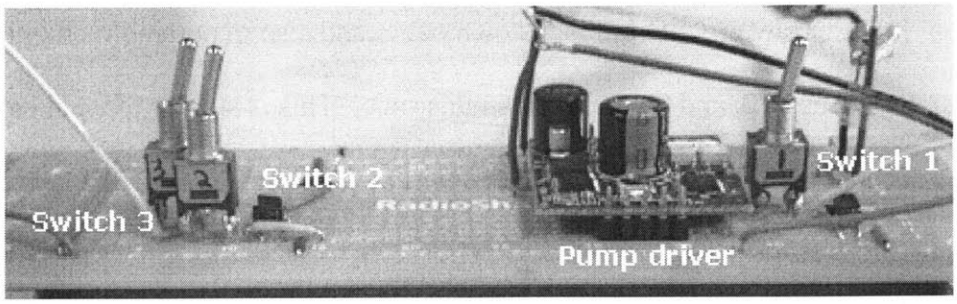

Figure 6-11 Close-up of hybrid demo

6.3 Hybrid Demo States

Three different states can be shown by this demonstration.

6.3.1 Power from capacitor

In this state, as shown in Figure 6-12, a fully charged capacitor in the LED node, Capacitor 1, is powering the LED bulbs. Switch 3 is closed. As discussed in Section 6.2.3, the size of the capacitor has been selected such that it will fully power the bulb for approximately 1 second and then it will begin to dim. This state represents a state that is similar to the initial startup or slow acceleration of the car.

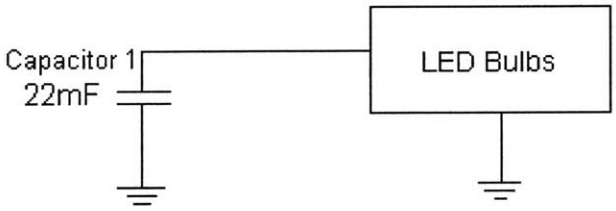

Figure 6-12 Power from capacitor

6.3.2 Power from capacitor and fuel cell

In this state, shown in Figure 6-13, the fuel cell is powering its own methanol pump, maintaining the charge of the capacitor in the fuel cell / pump node while also recharging the capacitor in the LED bulb node, and also powering the LED bulb

application. It has to power LED bulbs, its own pump and also maintain / recharge capacitors. Switches 1, 2, and 3 are closed in this state. This is similar to what happens during low speed cruising in a car: the fuel cell will kick in when it notices a decrease in capacitance.

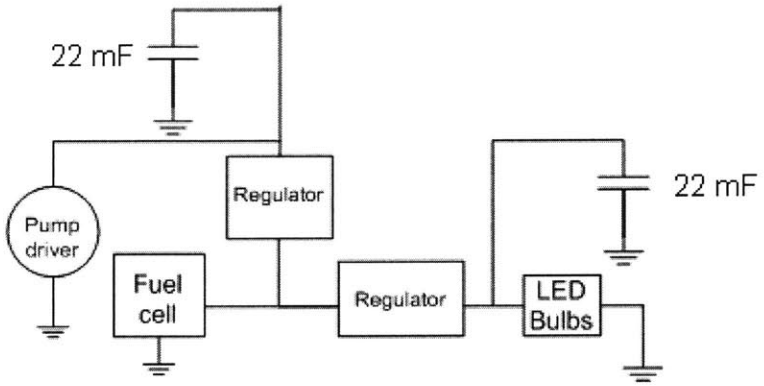

Figure 6-13 Power from capacitor and fuel cell

6.3.3 Power from fuel cell

In this state, as shown in Figure 6-14, the fuel cell is powering its own methanol pump, maintaining the charge of the capacitor in the fuel cell / pump node and also powering the LED bulbs. Switch 3 is opened and switches 1 and 2 remain closed. This is similar to high speed cruising when just the fuel cell would be powering the application.

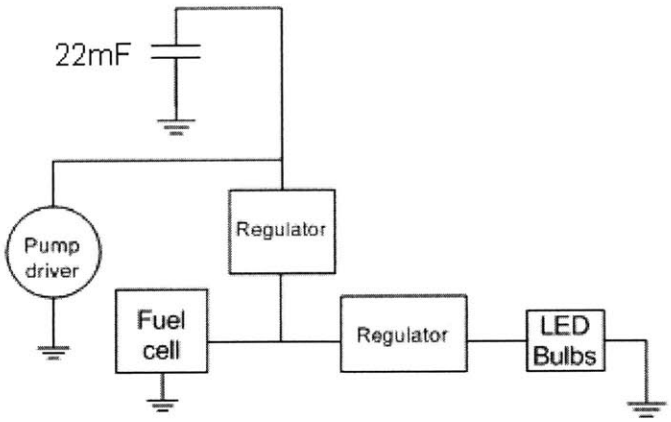

Figure 6-14 Power from fuel cell

CHAPTER

7 Conclusion

7.1 Summary

As mobile devices advance to 3G and beyond, there will be a pressing need for increased power to drive these devices. The projected performance growth rate of Li-Ion batteries is insufficient to provide the needed power for these upcoming devices, thus an alternative power source has been identified to fulfill the future needs: fuel cells. The direct methanol fuel cell has been identified as a promising candidate.

However, commercialization of mobile devices containing fuel cells has been difficult due to the several factors including inefficiencies in the fuel cell, large size, and difficulties of integration into the device. An Axiomatic approach was used to identify the key problems that prevent commercialization, along with possible solutions for these problems. These possible solutions were used to design and build a fuel cell for mobile devices of small size, high performance, and integrated hybrid circuitry.

A passive cathode fuel cell, created by replacing the typical cathode graphite plate with a copper wire mesh reinforced by a thin plate, eliminated a pump at the cathode and decreased the overall volume of the fuel cell.

Two inefficiencies in particular, the flooding at the cathode and methanol crossover, were identified as contributors to the low performance of DMFCs. To construct a high performance fuel cell, several experiments varying the methanol flow rate, oxygen and methanol concentration, and cathode GDL were performed on prefabricated MEAs in order to decrease flooding and methanol crossover.

The MEA from the Fuel Cell Store had higher performance than the MEA from ElectroChem Inc. In addition, increasing oxygen concentration improved performance, whereas increasing methanol concentration decreased performance due to methanol crossover effects. The effects of the change of methanol flow rates were negligible and using a plain carbon cloth was just as efficient as using carbon paper coated with an MPL.

In addition, an MEA was fabricated and modified using polyvinyl alcohol PVA to test its effect on decreasing methanol crossover for improved fuel cell performance. Prefabricated MEAs were compared to the experimentally fabricated MEAs that were created using the decal method. The experimentally fabricated MEAs had a much lower performance than the prefabricated MEAs, most likely due to the poor catalyst fabrication and/or application onto the membrane. However, it followed normal performance curve trends. Furthermore, the modified PVA/Nafion membrane showed improvement in preventing methanol crossover although it had decreased proton conductance.

Finally, a fuel cell – capacitor hybrid circuit demo was designed and demonstrated because in an actual mobile device, the fuel cell needs to be operated in hybrid with a battery or super capacitor of some sort.

7.2 Future work and Recommendation

The objective of this thesis was to create an integrated fuel cell unit for a mobile device that has small size, high performance, and incorporated with hybrid circuitry. Based on the research accomplishments of this thesis, there are 4 areas that have been identified for future research endeavors:

- increase oxygen concentration at the cathode
- further reduction of methanol crossover
- high volume manufacturing compatibility of MEAs
- battery-fuel cell hybrid technology

Experiments performed with the passive fuel cell and the prefabricated MEA followed normal performance curve trends. However, at power densities of approximately 5 mW/cm^2, for a 5 cm^2 active area MEA, the current single MEA fuel cell can only provide approximately 40mW of power. A multicell fuel cell created from this MEA, that has for example, 5 cells, could produce 200mW of power from the prefabricated MEAs inside the constructed passive fuel cell. This is unfortunately not enough to power the future 3G mobile devices, which have been estimated to need at least 2W of power [1]. The results suggested that increasing oxygen concentration would increase the performance. A way to do this without significantly increasing volume is to increase the partial pressure of oxygen. It would be worthwhile to pursue various methods of increasing partial pressure of oxygen in air given a confined volume.

Furthermore, the results showed the decrease in performance due to methanol crossover and proved the need to continue pursuing methods to prevent it. Other chemicals that have good methanol selectivity should be further tested for its proton conductivity in order to create an MEA that would prevent methanol crossover without decreasing the overall performance of the fuel cell due to its poor ability to conduct protons. Other factors such as surface roughness of the membrane could be also be modified and tested to see if they can achieve this.

The experimentally fabricated MEA demonstrated even lower performance mainly due to the ineffective catalyst fabrication process. The catalyst fabrication process brings up issues involving high volume manufacturing compatibility of fuel cells in the future. It was discovered that current process of creating MEAs was a difficult and long process to learn and an even longer one to perfect. The current process used is slow and imprecise. Research to improve the speed and precision of the current MEA manufacturing process with possibly some degree of automation could be helpful when thinking about eventual full scale production of MEAs for future applications.

Future applications also require fuel cell – battery hybrid integration capacity. It would be important to design and construct a fuel cell – battery hybrid that could be automated with a microcontroller, which could sense the power needed by the device and turn the fuel cell and battery on and off appropriately. Finally, when thinking of making further changes in the fuel cell, it is essential to do this with an integrated approach.

References

1 "NTT DoCoMo develops prototype micro fuel cell for FOMA handsets," *NTT DoCoMo press release article*, Sept 30, 2004, Tokyo Japan: http://www.nttdocomo.com/pr/2004/001208.html

2 P. Kallender, "Mobile phone fuel cells coming in 2007," *PC World*, July 13, 2005: http://www.pcworld.com/resource/article/0,aid,121816,pg,1,RSS,RSS,00.asp

3 G. Makuch, "Fuel Cell firm's neat solution for batteries," *CNET news.com*, June 21, 2004: http://news.com.com/Fuel+cell+firms+neat+solution+for+batteries/2100-1005_3-5242559.html

4 J. Larmine, A. Dicks, *Fuel Cell Systems Explained*, Second Ed. John Wiley & Sons, 2003

5 S.M Haile, D.A. Boysen, C.R.I. Chisholm, R.B. Merle, "Solid acids as fuel cell electrolytes," *Letters to Nature*, Vol 410, 2001, p 910-913.

6 M.N. Tsampas, A. Pikos, S. Brosda, A. Katsaounis, C.G. Vayenas, "The effect of membrane thickness on the conductivity of Nafion," *Electrochimica Acta*, Vol 51, 2006, p 2743-2755.

7 J. Kim, S.M. Lee, S. Srinivasan, "Modeling of proton exchange membrane fuel cell performance with an empirical equation," *Electrochemical Society*, Vol 142, 2005, p 2670-2674.

8 G. Hoogers, *Fuel Cell Technology Handbook*, CRC Press, 2003.

9 X. Ren, S. Gottesfeld, "Electro-osmotic drag of water in poly(perfluorosulfonic acid) membranes," *Journal of Electrochemical Socity*, Vol 148, 2001, p A87-A93.

10 G.Q. Lu, F.Q. Liu, C.Y. Wang, "Water transport through Nafion 112 membrane in DMFCs," Electrochemical and Solid-State Letters, Vol 8, 2005, p A1-A4.

11 E. Peled, A. Blum, A. Aharon, M. Philosoph, Y. Lavi, "Novel approach to recycling water and reducing water loss in DMFCs," *Electrochemical and Solid-State Letters*, Vol 6, 2003, p A268-A271.

12 Z.G. Shao, X. Wang, I.M. Hsing, "Composite Nafion/polyvinyl alcohol membranes for the direct methanol fuel cell," *Journal of Membrane Science*, Vol 210, 2002, p147-153.

13 H. Wu, Y. Wang, "A methanol barrier polymer electrolyte membrane in direct methanol fuel cells," *Journal of New Materials for Electrochemical Systems*, Vol 5, 2002, p 251-254.

14 M.S. Kang, J.H. Kim, J Won, S.H. Moon, Y.S. Kang, "Highly charged proton exchange membranes prepared by using water soluble polymer blends for fuel cells," Journal of Membrane Science, Vol 247, 2005, p 127-135.

15 N.P. Suh, *Axiomatic Design: Advances and Applications*, Oxford University Press, 2001.

16 E-TEK FAQ web page: http://www.etek-inc.com/faq/index.php

17 D. Carey, "Packaging aids 3G phone evolution," *Electronic Engineering Times*, Is 1400, 2005, p60.

18 A.K. Shuklua, P.A. Christensen, A.J Dickinson, A. Hamnett, "A liquid-feed solid polymer electrolyte direct methanol fuel cell operating at near-ambient conditions," *Journal of Power Sources*, Vol 76, 1998, 54-59.

19 F. Jaouen, S. Hassal, W.V. Wijngaart, A. Lundblad, G. Lindbergh, G. Stemme, "Adhesive copper films for an air-breathing polymer electrolyte fuel cell," *Journal of Power Sources,* Vol 144, 2005, p 113-121.

20 T. Shimizu, T. Momma, M. Mohamedi, T. Osaka, S. Sarangapani, "Design and fabrication of pumpless small direct methanol fuel cells for portable applications," *Journal of Power Sources*, Vol 147, 2004, 277-283.

21 M.S. Wilson, S. Gottesfeld, "Thin-film catalyst layers for polymer electrolyte fuel cell electrodes," Journal of Applied Electrochemistry, Vol 22, 1992, p 1-7.

22 S. Zumdahl, *Chemistry*, Houghton Mifflin,1989.

23 Images from: http://www.fueleconomy.gov/feg/hybridtech.shtml

24 LTC3525 User's Manual from Linear Technology.